Analytical insights into the partially integrated transport modeling method for hybrid Reynolds averaged Navier-Stokes equations-large eddy simulations of turbulent flows

Bruno Chaouat, Roland Schiestel

Analytical insights into the partially integrated transport modeling method for hybrid Reynolds averaged Navier-Stokes equations-large eddy simulations of turbulent flows

Bruno Chaouat[1,a)] and Roland Schiestel[2]
[1]*ONERA, 92322 Châtillon, France*
[2]*IRPHE, Château-Gombert, 13384 Marseille, France*

(Received 26 December 2011; accepted 9 July 2012; published online 31 August 2012)

The basis of the partially integrated transport modeling (PITM) method was introduced by Schiestel and Dejoan ["Towards a new partially integrated transport model for coarse grid and unsteady turbulent flow simulations," Theor. Comput. Fluid Dyn. **18**, 443 (2005)] and Chaouat and Schiestel ["A new partially integrated transport model for subgrid-scale stresses and dissipation rate for turbulent developing flows," Phys. Fluids **17**, 065106 (2005)]. This method provides a continuous approach for hybrid RANS-LES (Reynolds averaged Navier-Stokes equations-large eddy simulations) simulations with seamless coupling between RANS and LES regions. The main ingredient of the method is the new dissipation-rate equation that can be applied as a subfilter scale turbulence model. Then, it becomes easy to convert almost any usual RANS transport model into a subfilter scale model. In particular, the method can be applied to two equation models and to stress transport models as well. In the derivation of the method, the partial integration technique allows to keep a link between the spectral space and the physical space of the resulting model. The physical turbulent processes involving the production, dissipation, and flux transfer of the turbulent energy are introduced in the equations. The present work, after recalling the main building steps of the PITM method, brings further insight into the physical interpretation of the method, its underlying hypotheses and its internal acting mechanisms. In particular, the finiteness of the coefficients used in the dissipation-rate equation is discussed in detail from a theoretical point of view. Then, we consider the analytical example of self-similar turbulent flow for analyzing the dissipation-rate equation. From an analytical solution obtained by Taylor series expansions taking into account the Kovasznay hypothesis for evaluating the transfer term, we compute the functional coefficients c_{ϵ_2} and $c_{sfs\epsilon_2}$ used in RANS and LES methodologies, respectively, and we demonstrate that both coefficients take on finite values when the Reynolds number goes to infinity. Finally, after briefly mentioning some flow illustrations to get a real appraisal of the PITM method in its capabilities to simulate unsteady flows on relatively coarse grids with a sufficient accuracy for engineering computations, we study the coefficient $c_{sfs\epsilon_2}$ through one chosen example.
 [http://dx.doi.org/10.1063/1.4745003]

I. INTRODUCTION

The current trends in turbulence modeling for tackling engineering applications is to develop hybrid RANS-LES (Reynolds averaged Navier-Stokes equations-large eddy simulations) methods capable to reproduce a RANS-type behavior in the vicinity of a solid boundary and a LES-type

a) Author to whom correspondence should be addressed. Electronic mail: Bruno.Chaouat@onera.fr.

behavior far away from the wall boundaries.[1] As mentioned by Germano,[2] this type of approach allows to bridge the gap between the RANS and LES approaches. Indeed, these hybrid methods constitute a good compromise between the statistical RANS approach which is not well suited for simulating complex or unsteady flows subjected to a large range of frequencies that can interact with the turbulence time scales and a highly resolved LES approach that requires prohibitive computer time consumption. For instance, as mentioned by Spalart,[3,4] it will not be possible in a near future to simulate industrial applications requiring large computational domains like an entire aircraft, even with the rapid increase of super-computer power. The computational cost of such a flow simulation still remains not affordable. For a comparative assessment of RANS and LES methods, Gatski *et al.*[5] and Lesieur and Metais[6] have pointed out the respective advantages and drawbacks of both methods in some interesting review papers. According to the literature,[5,7] hybrid methods can be classified into two categories, zonal and non-zonal methods. This terminology employed for classifying hybrid RANS-LES methods among zonal and non-zonal methods can be, however, ambiguous since both methods use different models in different regions. For this reason, some authors[1] prefer to identify on the one hand segregated modeling when different models are used and, on the other hand unified modeling corresponding to the counterpart to segregated modeling considered as a more continuous approach. Among these hybrid RANS-LES methods, the detached eddy simulation[3,8] where the model is switching from a RANS behavior to a LES behavior, depending on a criteria based on the turbulent length-scale, is certainly one of the most popular models used for aeronautical applications. Generally speaking, although of practical use, the main shortcoming of standard hybrid RANS-LES methods comes from the connection interface between the RANS and LES regions where the turbulence closure changes from one model to another one without continuity when crossing the interface.[9,10] This procedure may require internal forcing in order to get the correct velocity and stress profiles in the boundary layer[11] and still pose some conceptual and numerical problems.

In the field of hybrid RANS-LES methods, Schiestel and Dejoan[12] and Chaouat and Schiestel[13] have developed in the last several years a partially integrated transport modeling (PITM) method with seamless coupling between the RANS and LES behaviors which is inspired from multiple-time scale modeling[14] developed previously in the RANS framework. This new approach is intended to respond to the problems raised by conventional hybrid RANS-LES methods. In particular, the PITM method allows to simulate turbulent flows on relatively coarse grids or flows with strong departure from spectral equilibrium. Such situations in flow physics occur, for instance, when forced unsteadiness interacts with the turbulence field, energy being injected into the flow,[12] but also in more complex situations where natural self-sustained unsteadiness develops due to the existence of organized eddies in particular flow geometries.[13,15] From this method, these authors have derived some subfilter turbulent models, a former using a viscosity two-equation model and the latter using a stress transport model based on second-moment closure. In contrast with zonal hybrid RANS-LES models, the models derived from the present PITM method have the particularity to vary continuously with respect to the ratio of the turbulent length-scale to the grid-size L_e/Δ (or the filter width) so that they avoid the need to set any interface between RANS and LES regions and to change the model from one computational domain to another one. Among these models, the subfilter scale stress transport models[13,16–19] transposed from Reynolds stress models (RSM) (Refs. 20–23) are probably the most elaborated models based on complex constitutive relations. Although the PITM method has been developed in the wave number space, it is possible to transpose its formalism in the frequency space. This work was done by several authors, Fadai-Ghotbi *et al.*[18] involved in the Poitier group in France. These authors have considered temporal filters instead of physical space filters to handle non-homogeneous stationary flows. Their method called TPITM (temporal partially integrated transport modeling) method was also used to derive the dissipation-rate equation in an analogous manner. As a result, they showed that the dissipation-rate equation finally takes the same formulation as the one found in the spectral space by the original PITM method. Another approach is the PANS (partially averaged Navier-Stokes) method[24] based on the self-similarity scale assumption that has recently emerged for performing unsteady computations. Although some equations of the PANS approach look similar to the PITM method, the method does not provide a clear link between the model equations and the filter size.

The PITM method is now becoming more widespread in turbulence modeling[13,17,19,25–27] because of its practical interest in the field of engineering applications. As the method retains a strong link with the underlying spectral concepts, there is a need to make clear how this connection is working. In the present work, we shall first briefly recall the basic principles and the foundation of the method. After this recalling of the main building steps of the PITM method, then we shall make a more in depth discussion of the underlying hypotheses, their physical interpretation and the acting mechanisms behind the equations, and so how the derived subfilter models work. We will present the partially integrated equations describing the physical turbulent processes involving the production, dissipation, and flux transfer of the partial turbulent energy associated to each spectral zone. These spectral balance equations constitute the cornerstone of the PITM method. In this formalism, we will introduce the cutoff wave number used in the spectrum splitting in LES by means of dimensionless relations and we will discuss their domain of validity from a theoretical point of view. We will show that the PITM method can be applied to almost any statistical model to derive its corresponding subfilter model that can be used in LES. The important question concerning the finiteness of the coefficients used in the dissipation equation will be extensively discussed. In particular, we will examine the asymptotic behavior of the functional coefficient $c_{sfs\epsilon_2}$ when the turbulence Reynolds number goes to infinity and we will give arguments to show that it reaches finite values whatever the flow considered. Then, we consider the given example of a self-similar turbulent flow. We will show that the generic dissipation-rate equation is physically consistent with this type of flow. To do this, we will calculate the analytical solution of Reid and Harris[28] obtained in the present case by means of Taylor series expansions developed in the spectral space taking into account the Kovasznay hypothesis for evaluating the transfer term. We will determine the expressions of the functional coefficients c_{ϵ_2} and $c_{sfs\epsilon_2}$ used in the statistical and subfilter generic dissipation-rate equations to show that these coefficients, as expected, take on finite values when the Reynolds number goes to infinity. Finally, after briefly mentioning some flow illustrations to get a real appraisal of the PITM method in its capabilities to simulate unsteady flows on relatively coarse grids, we will study the coefficient $c_{sfs\epsilon_2}$ through one chosen example.

II. THE SPECTRAL FRAMEWORK IN THE STATISTICAL SENSE

A. Spectral transport equations

A turbulent flow of a Newtonian viscous fluid is considered. The theoretical formalism of the dynamic of homogeneous turbulence in spectral space can be obtained from the transport equation of the two-point fluctuating velocity correlations in the physical space, by taking its Fourier transform.[29,30] Extending this methodology to non-homogeneous flows is possible[31,32] but leads to very complicated equations. The practical mean, however, to keep the equation reasonably simple and tractable is to introduce the approximate concept of tangent homogeneous space, that we used in the development of the PITM method.[14,33] In this approach, the variation of the mean velocities is accounted for by the use of Taylor series approximations limited to the linear terms. These equations are functions of the wavevector. They can be converted into one-dimensional spectral equation that is the only function of the wave number by averaging over spherical shells. This technique introduced by the French turbulence group in Lyon (see, for instance, Jeandel *et al.*[34] or Cambon *et al.*[35]) applied to the fluctuating field in homogeneous turbulence allows a considerable simplification of the mathematical formalism, although the directional information is lost. But this practice is a necessary surrender to keep simple equations and is sufficient for engineering applications. These spectral equations have been the basis of one-dimensional non-isotropic spectral models[34–37] and an interesting overview has been conducted in Ref. 38. Spectral turbulence transport equations are the basis to develop both multiple scale statistical models[14,39,40] and subfilter transport closures such as the PITM method.[12,13,33] As a result of the mathematical formalism,[14,33,34] the dynamic equation for the spectral two point velocity correlation tensor in one-dimensional spectral space formally reads

$$\frac{\partial \varphi_{ij}(\boldsymbol{X},\kappa)}{\partial t} = \mathcal{P}_{ij}(\boldsymbol{X},\kappa) + \mathcal{T}_{ij}(\boldsymbol{X},\kappa) + \Pi_{ij}(\boldsymbol{X},\kappa) + \mathcal{J}_{ij}(\boldsymbol{X},\kappa) - \mathcal{E}_{ij}(\boldsymbol{X},\kappa), \tag{1}$$

where the different terms appearing in the right-hand side of this equation are, respectively, the production, transfer, redistribution, diffusion, and dissipation contributions, acting in the spectral space associated to the scalar wave number κ (modulus of the wavevector). The exact expressions of these terms can be found for instance in Ref. 33. In this equation, the variable $\boldsymbol{X}$ denotes the midway position $\boldsymbol{X} = \frac{1}{2}(\boldsymbol{x}_A + \boldsymbol{x}_B)$ between the two points $\boldsymbol{x}_A$ and $\boldsymbol{x}_B$ introduced as the reference location in space. As already mentioned earlier, an essential simplification used in establishing Eq. (1) is the integration on spherical shells of modulus κ to get one-dimensional spectra such as $\varphi_{ij}(\boldsymbol{X}, \kappa) = \int_{|\boldsymbol{\kappa}|} \boldsymbol{\Phi}_{ij}(\boldsymbol{X}, \boldsymbol{\kappa}) d\boldsymbol{\kappa}$ in which the spectral tensor $\boldsymbol{\Phi}_{ij}(\boldsymbol{X}, \boldsymbol{\kappa})$ is depending on the full wavevector $\boldsymbol{\kappa}$, thus not only on the modulus but also on the orientation. Spherical averaging[33,39,40] allows to reduce the complexity of the problem in a reasonable way, especially in real flow applications in which the $\boldsymbol{X}$ dependency is important. It is worth mentioning here that similar approaches have been made in physical space for the two-point correlation functions. In this case, the correlation tensor is a function of $\boldsymbol{\xi} = \boldsymbol{x}_B - \boldsymbol{x}_A$, the vector joining the points A and B, but only the dependence on the modulus ξ is retained in spherically averaged structure functions. For instance, one can cite the recent work by Cimarelli and De Angelis[41] for turbulent wall flows in which r-averaging is performed on square domains in wall parallel planes, keeping the wall distance parameter. In the more theoretical case of homogeneous anisotropic turbulence, there is no $\boldsymbol{X}$ dependency in space and the turbulent diffusion terms vanish. Consequently, it becomes possible to further refine the analysis. The linear rapid transfer term and the pressure redistribution term present in Eq. (1) as rapid parts of the terms $\mathcal{T}_{ij}(\boldsymbol{X}, \kappa)$ and $\Pi_{ij}(\boldsymbol{X}, \kappa)$ need closure assumption while they would be already closed in the transport equation for $\boldsymbol{\Phi}_{ij}$. This lack of information on the directional dependence on the wavevector $\boldsymbol{\kappa}$ leads to a specific closure problem with solutions proposed in particular in the Lyon group in France[35,42] based on a linear analysis coupled with the extended eddy damped quasi-normal Markovian (EDQNM) approach[43,44] which is an outgrowth of the classical EDQNM analytical theory.[45] This dependency upon the full wavevector $\boldsymbol{\kappa}$ in the three-dimensional spectral space introduces another kind of anisotropy and has lead some authors to introduce the directional anisotropy in addition to the polarization anisotropy.[44] The structure based model of Kassinos and Reynolds[46] developed independently in CTR of Stanford is also based on the similar decomposition into so-called "componentality" and "dimensionality." These considerations bring new analytical complexities and are particularly relevant in rapidly rotating turbulent flows.[36] Such a type of modeling has been introduced by Cambon *et al.*[47] including in addition to the usual Reynolds stress transport equation, a separate transport equation for the directional anisotropy which appears in physical space as a hidden parameter of the turbulence field.

B. Spectrum splitting and partial integration

In the present approach, each flow variable ϕ is decomposed into a statistical mean value $\langle\phi\rangle$ and a fluctuating turbulent part ϕ' which is developed itself into several ranks m of fluctuating parts $\phi'^{(m)}$ of increasing wave numbers as follows:[13,14]

$$\phi = \langle\phi\rangle + \sum_{m=1}^{N} \phi'^{(m)}, \tag{2}$$

corresponding to an extended form of the Reynolds decomposition. The terms of the series are defined by partial integration of their generalized Fourier transform

$$\phi'^{(m)}(\boldsymbol{\xi}) = \int_{\kappa_{m-1}<|\boldsymbol{\kappa}|<\kappa_m} \widehat{\phi}'(\boldsymbol{\kappa}) \exp(j\boldsymbol{\kappa}\boldsymbol{\xi}) d\boldsymbol{\kappa}, \tag{3}$$

where $\widehat{\phi}'(\boldsymbol{\kappa})$ denotes Fourier transform of $\phi'(\boldsymbol{\xi})$ and κ_m is a series of evolving partitioning wave numbers and where $\boldsymbol{\xi}$ denotes the vector difference $\boldsymbol{\xi} = \boldsymbol{x}_B - \boldsymbol{x}_A$. For $m = 1$, this formalism allows to recover the usual Reynolds decomposition $\phi = \langle\phi\rangle + \phi'^{(1)}$ used in RANS modeling in which the integrated whole spectrum is modeled. For $m = 2$ or more, we find the kind of decomposition retained in the multiple-scale statistical models.[14] The particular case of the two-level decomposition $m = 2$ is most often used in practice. In multiple-scale statistical models, all the spectral ranges are modeled. In the case of large eddy simulations (studied in Sec. III), the previous definitions of

splitting can be viewed as a statistical filter.[48] This is also the two level decomposition which will be used in large eddy simulations where only one part of the spectrum containing the small eddies is modeled while the large eddies are explicitly simulated. Hence, the decomposition can be written as $\phi = \langle\phi\rangle + \phi^{<} + \phi^{>}$ with $\phi^{<} = \phi^{(1)}$ and $\phi^{>} = \phi^{(2)}$. The transport equation of the partial turbulent stresses $\tau_{ij}^{(m)}$ is obtained by partial integration of the spectral spectrum in the wave number ranges $[\kappa_{m-1}, \kappa_m]$.[14,33] The partial turbulent stress $\tau_{ij}^{(m)}$ is defined by

$$\tau_{ij}^{(m)} = \int_{\kappa_{m-1}}^{\kappa_m} \varphi_{ij}(\boldsymbol{X}, \kappa) d\kappa. \tag{4}$$

Keeping in mind that the wave numbers can be evolving in time, the integration of Eq. (1) over the range $[\kappa_{m-1}, \kappa_m]$ provides the transport equation for the partial turbulent stress $\tau_{ij}^{(m)}$:

$$\frac{\partial \tau_{ij}^{(m)}}{\partial t} = P_{ij}^{(m)} + F_{ij}^{(m-1)} - F_{ij}^{(m)} + \Psi_{ij}^{(m)} + J_{ij}^{(m)} - \epsilon_{ij}^{(m)}. \tag{5}$$

Each term in the right-hand side of Eq. (5) is the integral in the interval $[\kappa_{m-1}, \kappa_m]$ of the corresponding terms in Eq. (1), the details can be found in Refs. 14 and 33. The transfer terms also include the contribution coming from the left-hand side derivative,

$$F_{ij}^{(m)} = \mathcal{F}_{ij}^{(m)} - \varphi_{ij}(\boldsymbol{X}, \kappa) \frac{\partial \kappa_m}{\partial t}, \tag{6}$$

with

$$\mathcal{F}_{ij}^{(m)} = -\int_0^{\kappa_m} \mathcal{T}_{ij}(\boldsymbol{X}, \kappa) d\kappa. \tag{7}$$

In Eq. (5), it is implicitly supposed that $F_{ij}^{(0)} = 0$. The transport equation of the partial turbulent kinetic energy $k^{(m)}$ is simply obtained by tensorial contraction of equation (5):

$$\frac{\partial k^{(m)}}{\partial t} = P^{(m)} + F^{(m-1)} - F^{(m)} + J^{(m)} - \epsilon^{(m)} \tag{8}$$

with the following definitions

$$\mathcal{F}^{(m)} = -\int_0^{\kappa_m} \mathcal{T}(\boldsymbol{X}, \kappa) d\kappa, \tag{9}$$

and where

$$F^{(m)} = \mathcal{F}^{(m)} - E(\boldsymbol{X}, \kappa) \frac{\partial \kappa_m}{\partial t}, \tag{10}$$

where $E(\boldsymbol{X}, \kappa) = \frac{1}{2}\varphi_{ii}(\boldsymbol{X}, \kappa)$, $P^{(m)} = \frac{1}{2}P_{ii}^{(m)}$, $F^{(m)} = \frac{1}{2}F_{ii}^{(m)}$, $\mathcal{F}^{(m)} = \frac{1}{2}F^{(m)}$, $J^{(m)} = \frac{1}{2}J_{ii}^{(m)}$, and $\epsilon^{(m)} = \frac{1}{2}\epsilon_{ii}^{(m)}$. On a schematic point of view, in high Reynolds number turbulence, all the contributions $\epsilon_{ij}^{(m)}$ are negligible in all the wave number ranges $[\kappa_{m-1}, \kappa_m]$ except for the last one corresponding to the dissipation range which verifies the relation $\epsilon_{ij}^{(N+1)} = F_{ij}^{(N)}$. Obviously, each one point statistical variable ϕ_{ij} is obtained by integrating the whole spectrum and thus is also equal to the sum of each partial contribution $\phi_{ij}^{(m)}$ leading to the result,

$$\phi_{ij} = \sum_{m=1}^{N} \phi_{ij}^{(m)}, \tag{11}$$

and in particular, the total stress tensor τ_{ij} and the dissipation-rate tensor ϵ_{ij} verify $\tau_{ij} = \sum_{m=1}^{N} \tau_{ij}^{(m)}$ and $\epsilon_{ij} = \sum_{m=1}^{N} \epsilon_{ij}^{(m)}$. In the following, the variable $\boldsymbol{X}$ will be omitted to alleviate the presentation of the mathematical physics formalism. When the general equation (5) is applied to the particular range wave numbers $[0, \kappa_1]$, $[\kappa_1, \kappa_2]$, and $[\kappa_2, \infty[$, we get two scale models leading to the exact

partially integrated transport equations:

$$\frac{\partial \tau_{ij}^{(1)}}{\partial t} = P_{ij}^{(1)} - F_{ij}^{(1)} + \Psi_{ij}^{(1)} + J_{ij}^{(1)} - \epsilon_{ij}^{(1)}, \tag{12}$$

$$\frac{\partial \tau_{ij}^{(2)}}{\partial t} = P_{ij}^{(2)} + F_{ij}^{(1)} - F_{ij}^{(2)} + \Psi_{ij}^{(2)} + J_{ij}^{(2)} - \epsilon_{ij}^{(2)}, \tag{13}$$

and

$$F_{ij}^{(2)} = \epsilon_{ij}^{(3)} \approx \epsilon_{ij}. \tag{14}$$

We have supposed that the turbulence Reynolds number is large, so that $\tau_{ij}^{(3)}$ is negligible while $\epsilon_{ij}^{(1)} = \epsilon_{ij}^{(2)} \approx 0$ meaning that $\epsilon_{ij}^{(3)}$ corresponds in fact to the true dissipation-rate ϵ_{ij}. In the case of low turbulence Reynolds number, this schematic description is no longer valid so that all the terms appearing in Eqs. (13) and (14) have to be therefore kept as shown in Ref. 49. Equations (12)–(14) describe the turbulent processes acting in each particular zone $[0, \kappa_1]$, $[\kappa_1, \kappa_2]$, and $[\kappa_2, \infty[$ of the energy spectrum taking into account the transfer fluxes of the turbulent energy passing from one zone to a next zone and ensuring the continuity between each interface. These equations can be contracted leading to the transport equations of the turbulent energies in the wave number ranges $[0, \kappa_1]$ and $[\kappa_1, \kappa_2]$ as follows:

$$\frac{\partial k^{(1)}}{\partial t} = P^{(1)} - F^{(1)} + J^{(1)} - \epsilon^{(1)}, \tag{15}$$

$$\frac{\partial k^{(2)}}{\partial t} = P^{(2)} + F^{(1)} - F^{(2)} + J^{(2)} - \epsilon^{(2)}, \tag{16}$$

$$F^{(2)} = \epsilon^{(3)} \approx \epsilon. \tag{17}$$

Equations (12)–(14), as well as (15)–(17), constitute, respectively, the transport equations for the partial scale stresses and turbulent energies in the statistical sense. Hence, they will be transposed into filtered equations in LES methodology as it will be shown in Sec. III. Note that a full integration in the spectral space yields the again well-known one point equations,

$$\frac{\partial \tau_{ij}}{\partial t} = P_{ij} + \Psi_{ij} + J_{ij} - \epsilon_{ij}, \tag{18}$$

and

$$\frac{\partial k}{\partial t} = P + J - \epsilon. \tag{19}$$

C. The transfer rate equations

In RANS methodology, the wave numbers splitting was first introduced in the past decade by Schiestel[14] for developing multiple scale models in the framework of second moment closures. Because of the evolution of the turbulent characteristic scale and energy distribution in time and space, it was assumed that the splitting wave number is related to the local parameters $k^{(m)}$ and $F^{(m)}$ by the dimensional relation,

$$\kappa_m - \kappa_{m-1} = \alpha_m \frac{F^{(m)}}{(k^{(m)})^{3/2}}, \tag{20}$$

where α_m is a numerical constant. As pointed out by Schiestel in RANS modeling,[14] this practice allows the wave numbers κ_m to adapt themselves dynamically to the evolving energy spectrum distribution when for instance the energy distribution would concentrate or spread away from the

initial distribution. So, we insist on the fact that Eq. (20) is not by any way a closure hypothesis, although it has to be dimensionally correct. In principle, the splitting wave numbers could be chosen freely. But the choice of Eq. (20) is mainly to guarantee that the splitting wave numbers conform to the evolving spectrum and prevent aberrant location of the splitting during evolution of the flow. This choice proved to be the most useful but this is not the only possible way to do it.[39,40] Equation (10) involves the flux transfers. From this equation, it is possible to compute the derivative $\partial\kappa_m/\partial t$ of the wave number κ_m as

$$\frac{\partial \kappa_m}{\partial t} = \frac{\mathcal{F}(\kappa_m) - F(\kappa_m)}{E(\kappa_m)}. \tag{21}$$

Using then Eqs. (20) and (21), one can derive a formal transfer rate equation for each flux energy $F(\kappa_m)$ at high Reynolds number that reads[14,49]

$$\frac{dF^{(m)}}{dt} = \mathcal{C}_1^{(m)} \frac{F^{(m)} P^{(m)}}{k^{(m)}} + \mathcal{C}_2^{(m)} \frac{F^{(m)} F^{(m-1)}}{k^{(m)}} + \mathcal{C}_3^{(m)} \frac{\left(F^{(m)}\right)^2}{k^{(m)}} + \mathcal{C}_4^{(m)} \frac{F^{(m)} \epsilon^{(m)}}{k^{(m)}} + J_F^{(m)}, \tag{22}$$

where $\mathcal{C}_i^{(m)}$ are coefficients depending on the spectral slice. Equation (22) embedded the diffusion term $J_F^{(m)}$. The model is thus composed of a set of $m = 1$ to N equations for the partial energies or each partial stress of Eq. (5) coupled with m equations for the energy fluxes between each spectral slice. The splitting wave numbers vary dynamically in order to comply with the variations of the energy spectrum itself. As it will be seen in Sec. III, the same kind of technique will be used in the PITM method with the major difference that the first splitting wave number will be fixed by the given filter width.

III. SPECTRAL PARTITIONING FOR HYBRID RANS-LES METHODS

This section is devoted to the PITM method. Although the preceding transport equations are still formally valid, there are three fundamental important differences to take into account in LES methodology. First, the PITM method only uses two level decomposition involving a large scale resolved spectral zone and a smaller scale modeled spectral zone. Second, the splitting cutoff wave number κ_c is determined by the LES filter cutoff Δ and is no longer governed by Eq. (21) as usually made in RANS modeling. Third, the transport equations are written in a instantaneous form instead of a statistical form.

A. Subfilter scale stress transport equations

As it was indicated in Sec. II B, the definition of the splitting given in Eq. (3) viewed as a statistical filter[48] can also be appropriate for LES. The two level decomposition has to be used in PITM simulations where the small eddies range is modeled while the large eddies range is simulated numerically. Thus, this decomposition leads to $\phi = \langle\phi\rangle + \phi^< + \phi^>$ with

$$\phi^<(\boldsymbol{\xi}) = \int_{0<|\boldsymbol{\kappa}|<\kappa_c} \widehat{\phi}'(\boldsymbol{\kappa}) \exp(j\boldsymbol{\kappa}\boldsymbol{\xi}) d\boldsymbol{\kappa}, \tag{23}$$

and

$$\phi^>(\boldsymbol{\xi}) = \int_{\kappa_c<|\boldsymbol{\kappa}|<\infty} \widehat{\phi}'(\boldsymbol{\kappa}) \exp(j\boldsymbol{\kappa}\boldsymbol{\xi}) d\boldsymbol{\kappa}, \tag{24}$$

in which κ_c, here, denotes the first splitting wave number. Using these definitions, it is simple matter to see that the filtered variable $\bar{\phi}$ can be computed as $\bar{\phi} = \langle\phi\rangle + \phi^<$ which contains in fact both statistical mean and large eddies fluctuations whereas $\phi^>$ is the subfilter-scale fluctuation of the small eddies. In the PITM method,[12,13,33,50] the practical case of two splitting wave numbers $\kappa_c = \kappa_1$ and $\kappa_d = \kappa_2$ is considered. So, the averaged subfilter scale (SFS) stress associated to the wave number range $[\kappa_c, \kappa_d]$ is defined by $\langle(\tau_{ij})_{sfs}\rangle = \tau_{ij}^{(2)}$ and its transport equation is obtained from

Eq. (13):

$$\frac{\partial \langle (\tau_{ij})_{sfs} \rangle}{\partial t} = \langle (P_{ij})_{sfs} \rangle + \langle (\Psi_{ij})_{sfs} \rangle + \langle (J_{ij})_{sfs} \rangle - \langle (\epsilon_{ij})_{sfs} \rangle, \tag{25}$$

where in this equation, the approximations $\langle (P_{ij})_{sfs} \rangle = P_{ij}^{(2)} + F_{ij}^{(1)}$, $\langle (\Psi_{ij})_{sfs} \rangle = \Psi_{ij}^{(2)}$, $\langle (J_{ij})_{sfs} \rangle = J_{ij}^{(2)}$, $\epsilon_{ij}^{(2)} \approx 0$ are conceded at high Reynolds number. The averaged subfilter dissipation-rate tensor $\langle (\epsilon_{ij})_{sfs} \rangle$ associated to the wave number range $[\kappa_d, \infty]$ results from Eq. (14):

$$\langle (\epsilon_{ij})_{sfs} \rangle = \epsilon_{ij}^{(3)} \approx F_{ij}^{(2)}. \tag{26}$$

The energy fluxes appearing in these equations are defined by $F_{ij}^{(1)} = F_{ij}(\kappa_c)$ and $F_{ij}^{(2)} = F_{ij}(\kappa_d)$. The transport equation of the subfilter turbulent energy is simply obtained from Eq. (25) in its contracted form

$$\frac{\partial \langle k_{sfs} \rangle}{\partial t} = \langle P_{sfs} \rangle + \langle J_{sfs} \rangle - \langle \epsilon_{sfs} \rangle. \tag{27}$$

Closure of Eq. (25) needs to model the subfilter tensorial dissipation-rate $\langle (\epsilon_{ij})_{sfs} \rangle$ which is approached by 2/3 $\langle \epsilon_{sfs} \rangle \delta_{ij}$. The modeling of the dissipation-rate $\langle \epsilon_{sfs} \rangle$ is made in the present case by means of its transport equation. In LES methodology, the transport equations of the filtered turbulent quantities are evolving in time and space. By analogy with the statistical mean equations (25) and (27), the transport equations of the filtered quantities to be modeled can be written in term of central moments as[51]

$$\frac{D(\tau_{ij})_{sfs}}{Dt} = (P_{ij})_{sfs} + (\Psi_{ij})_{sfs} + (J_{ij})_{sfs} - \frac{2}{3}\epsilon_{sfs}\delta_{ij}, \tag{28}$$

$$\frac{Dk_{sfs}}{Dt} = P_{sfs} + J_{sfs} - \epsilon_{sfs}. \tag{29}$$

In these equations, D/Dt denotes the material derivative defined by $D/Dt = \partial/\partial t + \bar{u}_k \partial/\partial x_k$ where $\bar{\boldsymbol{u}}$ is the filtered velocity. The passage from the set of statistical equations (25) and (27) to the set of filtered equations (28) and (29) is not truly demonstrated in the mathematical sense but results from physical intuitive considerations although the reciprocity is formally verified.[13,33] The use of a spectral cutoff filter defined by Eqs. (23) and (24) has the advantage that the Leonard term in the momentum equations strictly vanishes. However, in the physical space calculations, in practice, the filter will be either a smooth bell shaped function or the discretization grid cell itself. In these latter cases, and when the cell size varies, a commutation error[52,53] will appear like in any LES calculation. So, in physical space the equations will only be approximate. To minimize the commutation error, it will then be safe to use slowly varying cell sizes.

B. The generic subfilter dissipation-rate transport equation

In LES methodology, the wave number κ_1 is identified as being the cutoff wave number κ_c which is the spectral filter size usually related to the grid cell size by $\kappa_c = \pi/\Delta$ so that it is assumed constant or slowly variable in the case of variable step size of the grid. The splitting κ_c is no longer given by Eq. (20) as for two-scale RANS modeling but it is fixed by the filter size or the step size defined by the user. On the other hand, the wave number κ_2 corresponds to the dissipative wave number κ_d which is located at the far end of the inertial range of the spectrum assuming that the energy pertaining to higher wave numbers is entirely negligible. But it is also located before the dissipative zone as shown in Figure 1 which describes the sketches of the energy density spectrum $E(\kappa)$, the spectral flux transfer $\mathcal{F}(\kappa)$, and the spectral transfer term $\mathcal{T}(\kappa)$ with respect to the wave number κ in the spectral space at high Reynolds number. This choice is simply inspired from the multiple scale modeling[14] in which this spectral splitting avoids to consider infinite limits and molecular viscosity effects in the far end of the spectrum. The low Reynolds number viscous effects will be treated empirically[49] afterwards. The splitting wave number κ_d in LES methodology is still related to the

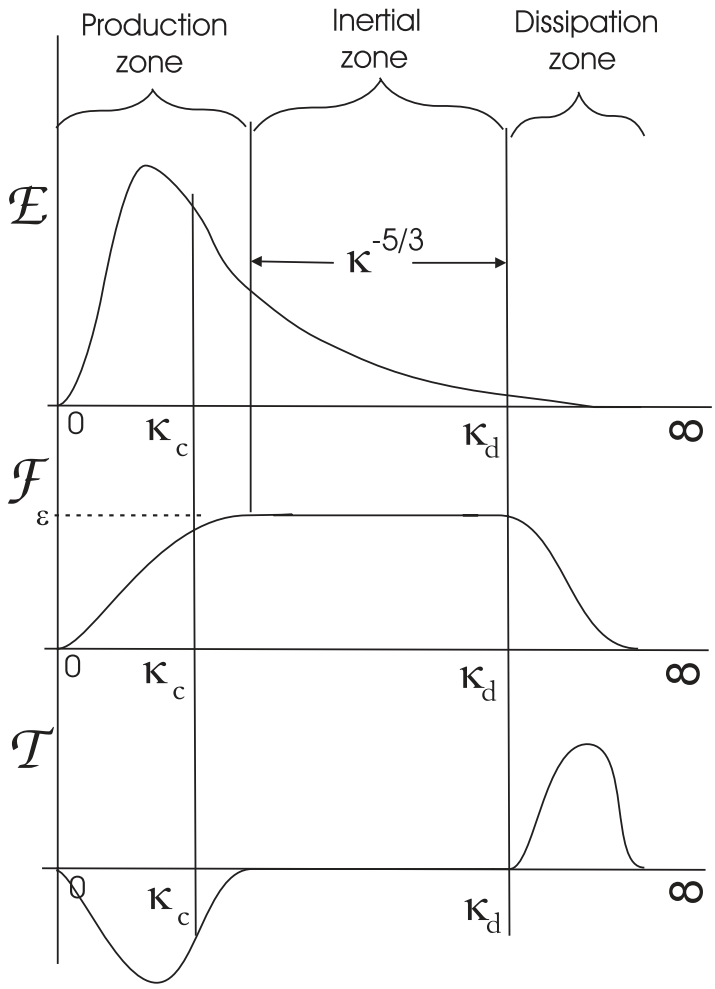

FIG. 1. Sketches of the energy density spectrum $E(\kappa)$, spectral flux transfer $\mathcal{F} = -\int_0^\kappa \mathcal{T}(\boldsymbol{X}, \kappa)d\kappa$, and spectral transfer term $\mathcal{T}$ with respect to the wave number κ in the spectral space, where κ_c denotes the cutoff wave number and κ_d is the dissipative wave number.

cutoff wave number κ_c by the dimensional relation (20) now written as

$$\kappa_d - \kappa_c = \zeta_c \frac{\langle \epsilon_{sfs} \rangle}{\langle k_{sfs} \rangle^{3/2}}, \tag{30}$$

where ζ_c is a given coefficient which may be dependent on the spectrum shape and on the Reynolds number. Like in multiple scale statistical models, Eq. (30) is introduced for conforming dynamically the location of the cutoff wave number to the evolving spectrum in time and space and consequently, it is not interpreted as a closure assumption. It simply results from a formal dimensional analysis of the turbulent variables k_{sfs} and ϵ_{sfs}. Obviously, here also, other choices than (30) could be possible as, for instance, those proposed by Schiestel.[39,40] From a physical point of view, the relation which links the wave numbers κ_c, κ_d, and the subfilter scale energy k_{sfs} is given by the definition of k_{sfs} itself

$$\langle k_{sfs} \rangle = \int_{\kappa_c}^{\kappa_d} E(\kappa)\, d\kappa. \tag{31}$$

In practice, κ_c can be located anywhere within the spectrum. So, Eq. (31) cannot be integrated using the inertial Kolmogorov law which is not satisfied in the general case, and consequently this equation cannot provide any explicit relation relying κ_c to κ_d. In the case of full statistical modeling where

$\kappa_c = 0$, Eq. (30) is reduced to equation,

$$\kappa_d = \zeta_d \frac{\epsilon}{k^{3/2}}, \tag{32}$$

where the coefficient ζ_d is a numerical constant chosen such that κ_d is located after the inertial range. This is an alternative method to derive an ϵ equation.[14] The subfilter dissipation-rate equation is then obtained by taking the derivative of Eq. (30) with respect to time using Eq. (10) written for the wave number κ_d:

$$\frac{\partial \kappa_d}{\partial t} = \frac{\mathcal{F}(\kappa_d) - F(\kappa_d)}{E(\kappa_d)} \tag{33}$$

considering also the transport equation (27) of the subfilter turbulent energy. The technique for deriving the ϵ equation is formally the same as the one used in statistical multiple scale modeling but there is an important difference. In statistical multiple scale models, all the splitting numbers κ_m are dynamically self adjusting to the spectrum evolution whereas in the LES case, the wave number κ_c is now a given quantity while κ_d still remains dynamically self adjusting. In the following, we will consider that both κ_c and κ_d are some functions of time to keep a general character of the formalism although the reader has to bear in mind that κ_c remains almost constant in time in the most usual LES applications. As a result of the algebra, it is then simple matter to see that the subfilter dissipation-rate equation in homogeneous turbulence reads[12,13]

$$\frac{\partial \langle \epsilon_{sfs} \rangle}{\partial t} = c_{sfs\epsilon_1} \frac{\langle \epsilon_{sfs} \rangle}{\langle k_{sfs} \rangle} \langle P_{sfs} \rangle - c_{sfs\epsilon_2} \frac{\langle \epsilon_{sfs} \rangle^2}{\langle k_{sfs} \rangle}, \tag{34}$$

where

$$c_{sfs\epsilon_1} = 3/2, \tag{35}$$

and

$$c_{sfs\epsilon_2} = \frac{3}{2} - \frac{\langle k_{sfs} \rangle}{(\kappa_d - \kappa_c) E(\kappa_d)} \left[\left(\frac{\mathcal{F}(\kappa_d) - F(\kappa_d)}{\langle \epsilon_{sfs} \rangle} \right) - \frac{E(\kappa_d)}{E(\kappa_c)} \left(\frac{\mathcal{F}(\kappa_c) - F(\kappa_c)}{\langle \epsilon_{sfs} \rangle} \right) \right]. \tag{36}$$

We have thus obtained formally the so-called generic dissipation equation because it is written in non-closed form. Setting $\kappa_d \gg \kappa_c$, and $E(\kappa_d) \ll E(\kappa_c)$, Eq. (36) reduces to

$$c_{sfs\epsilon_2} = \frac{3}{2} - \frac{\langle k_{sfs} \rangle}{\kappa_d E(\kappa_d)} \left(\frac{\mathcal{F}(\kappa_d) - F(\kappa_d)}{\langle \epsilon_{sfs} \rangle} \right). \tag{37}$$

Considering that we deal here with high Reynolds number turbulence, the relation $F(\kappa_d) = \langle \epsilon_{sfs} \rangle$ is nothing else than ϵ. In a compact form, Eq. (37) can be written as

$$c_{sfs\epsilon_2} = \frac{3}{2} - \frac{\langle k_{sfs} \rangle}{k} \zeta(\kappa_d), \tag{38}$$

where the function ζ is defined by

$$\zeta(\kappa_d) = \frac{k}{\kappa_d E(\kappa_d)} \left(\frac{\mathcal{F}(\kappa_d) - F(\kappa_d)}{\epsilon} \right). \tag{39}$$

At this stage, there are two possible approaches to close this equation. The first one is to try to use spectral theories in order to express the spectral fluxes $\mathcal{F}(\kappa_d)$ and $F(\kappa_d)$ appearing in Eq. (37) with known quantities. This is a difficult way leading to complex equations not tractable for engineering applications. The second approach is to give directly an estimate of the coefficients appearing in Eq. (34). This is the second approach that has been retained in the PITM method because it is far simple, even if some weaknesses are non avoidable. As an additional result of interest, one can notice that Eq. (37) reduces to $c_{sfs\epsilon_2} = 3/2$ in two particular cases. The first case occurs when $\kappa_d - \kappa_c \approx 0$ implying that the subfilter energy $\langle k_{sfs} \rangle$ in the slide $[\kappa_c, \kappa_d]$ is evanescent (see Appendix A). The second case corresponds to the exact spectral equilibrium when $\mathcal{F}(\kappa) = F(\kappa)$.

IV. THE PITM CLOSURE OF THE DISSIPATION-RATE EQUATION

The method followed for closing the dissipation-rate equation relies on two main requirements.[12,13] The first one is to impose that the subfilter model is consistent with its companion statistical model when κ_c goes to zero. We will see that this condition will imply that the $c_{sfs\epsilon_2}$ coefficient becomes a linear function of ratio $\langle k_{sfs}\rangle/k$. The second one is to estimate this ratio $\langle k_{sfs}\rangle/k$ analytically to achieve the closure. These two steps will be considered in the following sections.

A. Hypothesis of consistency with the RANS model at the zero cutoff limit

The generic dissipation-rate equation (34) using the relations (35), (38) and (39) is valid for any choice of κ_c because the spectral fluxes and dissipation-rate remain physically unchanged when the splitting κ_c in modified. This is also verified for the particular case $\kappa_c = 0$ corresponding to the full statistical case. So, for $\kappa_c = 0$, Eq. (38) reduces to

$$c_{\epsilon_2} = \frac{3}{2} - \zeta(\kappa_d), \tag{40}$$

the other relations remaining formally unchanged. By substituting Eq. (40) into Eq. (38), it is simple matter to see that the hypothesis of consistency with the RANS model in the zero cutoff limit leads to the resulting coefficients

$$c_{sfs\epsilon_1} = c_{\epsilon_1} = 3/2, \tag{41}$$

and

$$c_{\epsilon_{sfs2}} = \frac{3}{2} + \frac{\langle k_{sfs}\rangle}{k}\left(c_{\epsilon_2} - \frac{3}{2}\right). \tag{42}$$

The value suggested for c_{ϵ_1} seems restrictive if one remarks that this coefficient may take on different values in statistical RANS models according to its calibration made by different authors. Although the 3/2 value seems realistic as shown in Appendix A, this restriction can be easily removed if we want an exact compatibility with a given RANS model. In this aim, let us now consider the standard form of the statistical dissipation-rate equation written in homogeneous turbulence that reads

$$\frac{\partial \epsilon}{\partial t} = c_{\epsilon_1}\frac{\epsilon}{k}P - c_{\epsilon_2}\frac{\epsilon^2}{k} \tag{43}$$

with given values of the coefficients c_{ϵ_1} and c_{ϵ_2}. The issue to address is to compute the function $c_{sfs\epsilon_2}$ when the coefficient $c_{sfs\epsilon_1}$ differs from the value 3/2. Using Eqs. (38) and (40), respectively, then, Eqs. (34) and (43) can be rewritten in the following forms as

$$\frac{\partial\langle\epsilon_{sfs}\rangle}{\partial t} = c_{\epsilon_1}\frac{\langle\epsilon_{sfs}\rangle}{\langle k_{sfs}\rangle}\langle P\rangle_{sfs} - \left[\left(\frac{3}{2} - \frac{\langle k_{sfs}\rangle}{k}\zeta(\kappa_d)\right) - \left(\frac{3}{2} - c_{\epsilon_1}\right)\frac{\langle P_{sfs}\rangle}{\langle\epsilon_{sfs}\rangle}\right]\frac{\langle\epsilon_{sfs}\rangle^2}{\langle k_{sfs}\rangle} \tag{44}$$

and

$$\frac{\partial \epsilon}{\partial t} = c_{\epsilon_1}\frac{\epsilon}{k}P - \left[\left(\frac{3}{2} - \zeta(\kappa_d)\right) - \left(\frac{3}{2} - c_{\epsilon_1}\right)\frac{P}{\epsilon}\right]\frac{\epsilon^2}{k} \tag{45}$$

showing that

$$c_{\epsilon_2} = \left(\frac{3}{2} - \zeta(\kappa_d)\right) - \left(\frac{3}{2} - c_{\epsilon_1}\right)\frac{P}{\epsilon} \tag{46}$$

and

$$c_{sfs\epsilon_2} = \left(\frac{3}{2} - \frac{\langle k_{sfs}\rangle}{k}\zeta(\kappa_d)\right) - \left(\frac{3}{2} - c_{\epsilon_1}\right)\frac{\langle P_{sfs}\rangle}{\langle\epsilon_{sfs}\rangle} \tag{47}$$

Both Eqs. (46) and (47) allow to determine the function $\zeta(\kappa_d)$ in two different forms as follows:

$$\zeta(\kappa_d) = \left[\frac{3}{2} - c_{\epsilon_2} + \left(c_{\epsilon_1} - \frac{3}{2}\right)\frac{P}{\epsilon}\right], \tag{48}$$

and

$$\zeta(\kappa_d) = \left[\frac{3}{2} - c_{sfs\epsilon_2} + \left(c_{\epsilon_1} - \frac{3}{2}\right)\frac{\langle P_{sfs}\rangle}{\langle \epsilon_{sfs}\rangle}\right]\frac{k}{\langle k_{sfs}\rangle}. \tag{49}$$

By identifying Eq. (48) with Eq. (49), one can easily find the expression for the coefficient $c_{sfs\epsilon_2}$ that reads

$$c_{sfs\epsilon_2} = c_{\epsilon_2} + \left(\frac{3}{2} - c_{\epsilon_2}\right)\left[1 - \frac{\langle k_{sfs}\rangle}{k}\right] + \left(c_{\epsilon_1} - \frac{3}{2}\right)\left[\frac{\langle P_{sfs}\rangle}{\langle \epsilon_{sfs}\rangle} - \frac{P}{\epsilon}\frac{\langle k_{sfs}\rangle}{k}\right]. \tag{50}$$

If we assume that the ratio $\langle k_{sfs}\rangle/k$ of the subfilter energy to the total energy is constant or varies slowly with time, then

$$\frac{\partial}{\partial t}\left(\frac{\langle k_{sfs}\rangle}{k}\right) = \frac{\langle k_{sfs}\rangle}{k}\left(-\frac{1}{k}\frac{\partial k}{\partial t} + \frac{1}{\langle k_{sfs}\rangle}\frac{\partial \langle k_{sfs}\rangle}{\partial t}\right) \approx 0 \tag{51}$$

implying

$$\frac{\langle k_{sfs}\rangle}{k} \approx \frac{\partial \langle k_{sfs}\rangle}{\partial t}\frac{\partial t}{\partial k} = \frac{\langle P_{sfs}\rangle - \langle \epsilon_{sfs}\rangle}{P - \epsilon}. \tag{52}$$

Equation (52) allows to compute the ratio $\langle P_{sfs}\rangle/\langle \epsilon_{sfs}\rangle$ as follows:

$$\frac{\langle P_{sfs}\rangle}{\langle \epsilon_{sfs}\rangle} \approx 1 + \frac{\langle k_{sfs}\rangle}{k}\frac{P - \epsilon}{\epsilon}. \tag{53}$$

By substituting this ratio into Eq. (50), we obtain the final form of the coefficient $c_{sfs\epsilon_2}$ that reads

$$c_{sfs\epsilon_2} = c_{\epsilon_1} + \frac{\langle k_{sfs}\rangle}{k}(c_{\epsilon_2} - c_{\epsilon_1}). \tag{54}$$

Equation (54) established at high Reynolds numbers is the key equation for the PITM method. This new development clearly shows that the subfilter coefficient $c_{sfs\epsilon_2}$ can be adapted to any RANS dissipation-rate equation of the form (43) whatever the values of the coefficients c_{ϵ_1} and c_{ϵ_2} considered, and in particular when c_{ϵ_1} differs from the value 3/2. In that sense, this approximate derivation of Eq. (54) provides some justification of the practices already made in previous works.[13,16,33] So, we have proved in this section that the PITM method can be applied to almost any statistical transport model to derive its corresponding counterpart companion subfilter model and Eq. (44) is finally rewritten in its general form as

$$\frac{\partial \langle \epsilon_{sfs}\rangle}{\partial t} = c_{\epsilon_1}\frac{\langle \epsilon_{sfs}\rangle}{\langle k_{sfs}\rangle}\langle P_{sfs}\rangle - c_{sfs\epsilon_2}\frac{\langle \epsilon_{sfs}\rangle^2}{\langle k_{sfs}\rangle}. \tag{55}$$

At this step, it is of importance to note that Eq. (55) is related to the subfilter spectral interval $[\kappa_c, \infty[$ and that the first term appearing in the right-hand side of Eq. (55) involving the energy flux $\langle P_{sfs}\rangle$ passing through the cutoff wave number obviously depends on the location of κ_c. The second term appearing in the right-hand side of this equation also depends on the wave number κ_c through the coefficient $c_{sfs\epsilon_2}$ which is a function of the ratio $\langle k_{sfs}\rangle/k$. As a consequence, these terms are shown to balance each other, allowing to recover a subfilter dissipation-rate value which is practically independent of κ_c, at least at high Reynolds number, according to the theoretical physics of the turbulence cascade. This result is physically consistent with the fact that the dissipation-rate can be interpreted as a spectral flux energy passing through the dissipative wave number κ_d as shown by Eq. (26) written in its contracted form.

B. The analytical closure for the $c_{sfs\epsilon_2}$ term

The ratio $\langle k_{sfs}\rangle/k$ appearing in Eq. (54) is evaluated by means of an accurate energy spectrum $E(\kappa)$ inspired from a Von Kármán like spectrum

$$E(\kappa) = \frac{\frac{2}{3}\beta_\eta L_e^3\, k\, \kappa^2}{[1 + \beta_\eta(\kappa\, L_e)^3]^{11/9}}, \tag{56}$$

where β_η is a constant coefficient and L_e denotes the turbulent macro-scale leading to the result[16]

$$\langle k_{sfs}\rangle(\kappa_c) = \int_{\kappa_c}^{\infty} E(\kappa)\, d\kappa = k[1 + \beta_\eta(\kappa_c\, L_e)^3)]^{-2/9}. \tag{57}$$

So that the function $c_{sfs\epsilon_2}$ is given by

$$c_{sfs\epsilon_2}(\eta_c) = c_{\epsilon_1} + \frac{c_{\epsilon_2} - c_{\epsilon_1}}{\left[1 + \beta_\eta\, \eta_c^3\right]^{2/9}}, \tag{58}$$

where $\eta_c = \kappa_c L_e$ is a dimensionless parameter involving the cutoff wave number $\kappa_c = \pi/\Delta$ computed from the filter width (in practice the grid spacing) Δ and the turbulent macro-scale itself computed as $L_e = k^{3/2}/(\langle\epsilon_{sfs}\rangle + \langle\epsilon^<\rangle)$ built by means of the total turbulent energy and the total dissipation-rate $\epsilon = \langle\epsilon_{sfs}\rangle + \langle\epsilon^<\rangle$, including the dissipation in the subgrid zone ϵ_{sfs} and the resolved part of the dissipation-rate. Indeed, in many practical cases, the Reynolds number is finite, and it proved to be useful and closer to reality to include also the resolved part of the dissipation-rate in the scale definition. The resulting expression for η_c is

$$\eta_c = \kappa_c L_e = \frac{\pi\, k^{3/2}}{\Delta\,(\langle\epsilon_{sfs}\rangle + \langle\epsilon^<\rangle)}. \tag{59}$$

In Eq. (59), the resolved dissipation-rate caused by the large-scale fluctuating velocities $u_i^< = \bar{u}_i - \langle u_i\rangle$ is defined by

$$\epsilon^< = \nu\, \overline{\frac{\partial u_i^<}{\partial x_j}\frac{\partial u_i^<}{\partial x_j}}. \tag{60}$$

It allows to account even partly for low Reynolds number flow effects. But if the resolved part of the dissipation becomes important, this means that a low Reynolds number formulation of the model needs to be used. In Eq. (59), the quantity Δ is the effective filter usually obtained from $\Delta = (\Delta_1\Delta_2\Delta_3)^{1/3}$ where Δ_1, Δ_2, and Δ_3 are the filter width in each direction of space or in practice the grid step size in each direction of space. When the grid cell is very anisotropic like in wall flows, it is possible to account for this anisotropy of the grid like in the proposal of Scotti *et al.*[54]

$$\Delta = \Delta_a\left(\zeta + (1-\zeta)\frac{\Delta_b}{\Delta_a}\right), \tag{61}$$

where the filters Δ_a and Δ_b are defined by $\Delta_a = (\Delta_1\Delta_2\Delta_3)^{1/3}$ and $\Delta_b = [(\Delta_1^2 + \Delta_2^2 + \Delta_3^2)/3]^{1/2}$ and where ζ is a constant parameter. The theoretical value of the coefficient β_η appearing in Eq. (58) is obtained by the limiting condition $\lim_{\kappa\to\infty} E(\kappa) = C_\kappa\epsilon^{2/3}\kappa^{-5/3}$ for recovering the Kolmogorov law at high wave numbers. As a result, one can find $\beta_{\eta_T} = [2/(3C_\kappa)]^{9/2}$. It is worth noting that the analytical energy ratio obtained from Eq. (57), i.e.,

$$\left(\frac{\langle k_{sfs}\rangle}{k}\right)_{eq} = [1 + \beta_\eta(\kappa_c\, L_e)^3)]^{-2/9} \tag{62}$$

is an equilibrium value. In practice, the effective value of $\langle k_{sfs}\rangle/k$ during the numerical simulation can be different from its equilibrium values if there are some departures from equilibrium state. So, the $c_{sfs\epsilon_2}$ term can be more or less understood like a "return to equilibrium" term such as the Rotta term was a "return to isotropy" term. The present section allows to point out some essential differences with the PANS method cited in the introduction. In the PANS method,[24] the partial averaging is directly quantified using the unresolved-to-total ratio $f_k = \langle k_{sfs}\rangle/k$ for turbulence kinetic energy and $f_\epsilon = \langle\epsilon_{sfs}\rangle/\epsilon$ for dissipation which are empirically prescribed in each computation. The PANS equations can be derived very simply from an hypothesis of given constant ratios f_k and f_ϵ implying some self-similarity evolution hypothesis which is not relevant for all applications and specifically for flows in situation of out of spectral equilibrium turbulence. In spite of a totally different background, developed independently from each other, the PITM and PANS equations are hopefully very similar. However, the PITM approach provides a physical foundation in spectral space that allows to make a clear link between the unresolved-to-total ratios and the filter length scale

whereas the PANS in the contrary does not at all address this question. So, in a PITM simulation, although the filter width is prescribed as usually made in LES, the unresolved-to-total ratios are not prescribed but are obtained as a result of the calculation itself.

C. On the finiteness of the $c_{sfs\epsilon_2}$ term

The expression (37) for the $c_{sfs\epsilon_2}$ coefficient appearing in the generic dissipation-rate equation deserves a particular attention. The main questions being, does this term remains finite in all cases? And is it acceptable to model this term as a linear function of $\langle k_{sfs}\rangle$ with a constant factor? First of all, one has to notice that Eq. (10) applied for the wave number κ_d leading to Eq. (33) indicates that the energy flux $F(\kappa_d)$ passing through the wave number κ_d is composed by two terms of different origins, on the one hand the usual spectral transfer rate $\mathcal{F}(\kappa_d)$ and, on the other hand, an extra term corresponding to the variation of the κ_d splitting

$$F(\kappa_d) = \mathcal{F}(\kappa_d) - E(\kappa_d)\frac{\partial \kappa_d}{\partial t}. \tag{63}$$

So, it appears that the flux difference $F(\kappa_d) - \mathcal{F}(\kappa_d)$ is a driving mechanism in the variation of the dissipation-rate. More precisely, one can wonder what is the asymptotic limit of the coefficient $c_{sfs\epsilon_2}$ when the splitting wave number κ_d goes to infinity? This question can be raised when the turbulent Reynolds number goes to infinity and is of importance for the theoretical consistency of the method. Large Reynolds numbers may appear, for instance, when the molecular viscosity is very low. This situation is illustrated in Figures 2 and 3 showing the sketches of the spectral flux transfer $\mathcal{F}$ and the spectral transfer term $\mathcal{T}$, respectively, at very high turbulent Reynolds numbers for situations of spectral equilibrium and non-equilibrium flows. This high Reynolds number asymptotic limit is obtained in the present model by extending the inertial zone and increasing the wave number κ_d, thus moving farther the last spectral dissipative slice in the spectrum located just after κ_d as illustrated in the sketches of Figures 2 and 3. From a physical point of view, as the wave number κ_d increases, the inertial cascade zone becomes larger and larger so that an equilibrium zone finally will be established after a relaxation time at the large wave number κ_d implying therefore that the energy transferred from the inertial zone to the small scales will balance the dissipation-rate, i.e., $\mathcal{F}(\kappa_d) \approx \epsilon$. In the PITM method, the splitting wave number κ_c is constrained by Eq. (32), and then keeps a finite value. Consequently, $c_{sfs\epsilon_2}$ is obviously finite. It is, however, permissible to let the wave number κ_d go to infinity. This condition is obtained by taking the limiting condition $\zeta_c \to \infty$ in Eq. (30)

$$\kappa_d = \kappa_c + \lim_{\zeta_c \to \infty} \zeta_c \frac{\langle \epsilon_{sfs}\rangle}{\langle k_{sfs}\rangle^{3/2}}. \tag{64}$$

The $c_{sfs\epsilon_2}$ coefficient written in its generic form (no model) given by Eq. (37) can be computed by the energy spectrum $E(\kappa_d)$ approximated itself by the Kolmogorov law $E(\kappa) = C_\kappa \epsilon^{2/3}\kappa^{-5/3}$ where C_κ is the Kolmogorov constant yielding

$$c_{sfs\epsilon_2} = \frac{3}{2} - \frac{\langle k_{sfs}\rangle}{C_\kappa \epsilon^{2/3}\kappa_d^{-2/3}}\left(\frac{\mathcal{F}(\kappa_d) - \epsilon}{\epsilon}\right). \tag{65}$$

When $\kappa_d \to \infty$, the first factor appearing in the second term in the right-hand side of this equation goes to infinity while the second factor goes to zero because $\mathcal{F}(\kappa_d) \to \epsilon$. As a consequence, the limit of the second term takes the indeterminate form $0 \times \infty$. This does not mean at all that the limit is not finite as it was erroneously said in Ref. 55. In fact, Eq. (47) of Ref. 55 is not exact.

Moreover, in case of strict equilibrium implying that $\mathcal{F}(\kappa_d) = \epsilon$, Eq. (65) leads to the result $c_{sfs\epsilon_2} = 3/2$. At a first glance, this result may seem surprising. But one can remark that this situation also occurs in the usual statistical ϵ equation for homogeneous turbulence. Indeed, one has to bear in mind that a steady equilibrium turbulence can only exist if the production of the turbulence balances the dissipation-rate ($P = \epsilon$) and in addition if the constraint $c_{\epsilon 1} = c_{\epsilon 2}$ is satisfied in the dissipation-rate equation. In the general case, there are no strict equilibrium $\mathcal{F}(\kappa_d) \neq \epsilon$, and it is necessary to

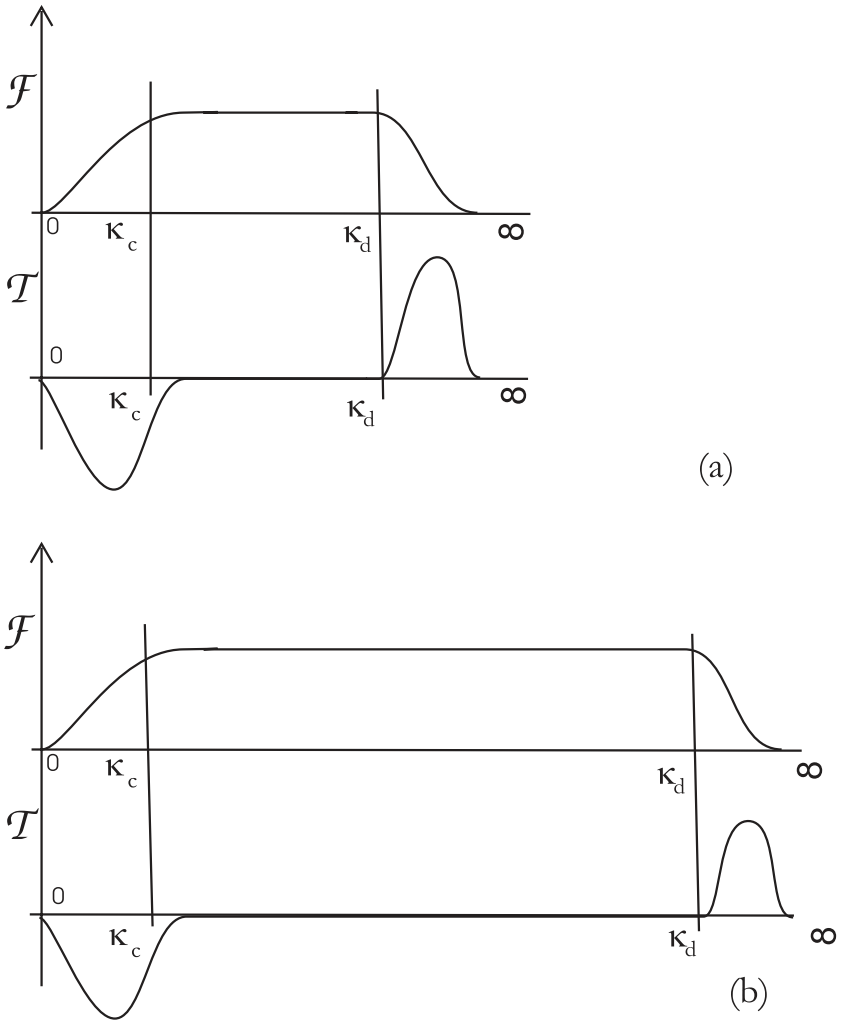

FIG. 2. Sketches of the spectral flux transfer $\mathcal{F}$ and spectral transfer term $\mathcal{T}$ with respect to the wave number κ in the spectral space for flows in spectral equilibrium. (a) High Reynolds number; (b) infinite Reynolds number.

make some spectral closure approximation to go further in the analysis. With this aim, let us suppose that the spectral transfer is approximated by the Kovasznay closure $\mathcal{F}(\kappa_d) = C_\kappa^{-3/2} E^{3/2} \kappa_d^{5/2}$. The question is to search a possible spectral distribution that could make the second term appearing in the right-hand side of Eq. (65) a constant quantity C_0 such as

$$C_0 = \frac{3}{2} - c_{sfs\epsilon_2} = \frac{\langle k_{sfs} \rangle}{C_\kappa \epsilon^{2/3} \kappa_d^{-2/3}} \left(\frac{C_\kappa^{-3/2} E^{3/2} \kappa_d^{5/2} - \epsilon}{\epsilon} \right). \tag{66}$$

From Eq. (66), one can easily deduce that

$$E(\kappa) \approx C_\kappa \epsilon^{2/3} \kappa_d^{-5/3} \left[1 + \frac{2}{3} C_0 \frac{C_\kappa \epsilon^{2/3} \kappa_d^{-2/3}}{\langle k_{sfs} \rangle} \right]. \tag{67}$$

Equation (67) suggests that the energy spectrum varies with respect to the wave number κ according to the form as

$$E(\kappa) \approx \alpha \kappa_d^{-5/3} + \beta \kappa_d^{-7/3}, \tag{68}$$

which is entirely plausible. Consequently, it is found that the coefficient $c_{sfs\epsilon_2}$ can indeed take on a finite value even if the wave number κ_d goes to infinity. From the previous discussions, one can

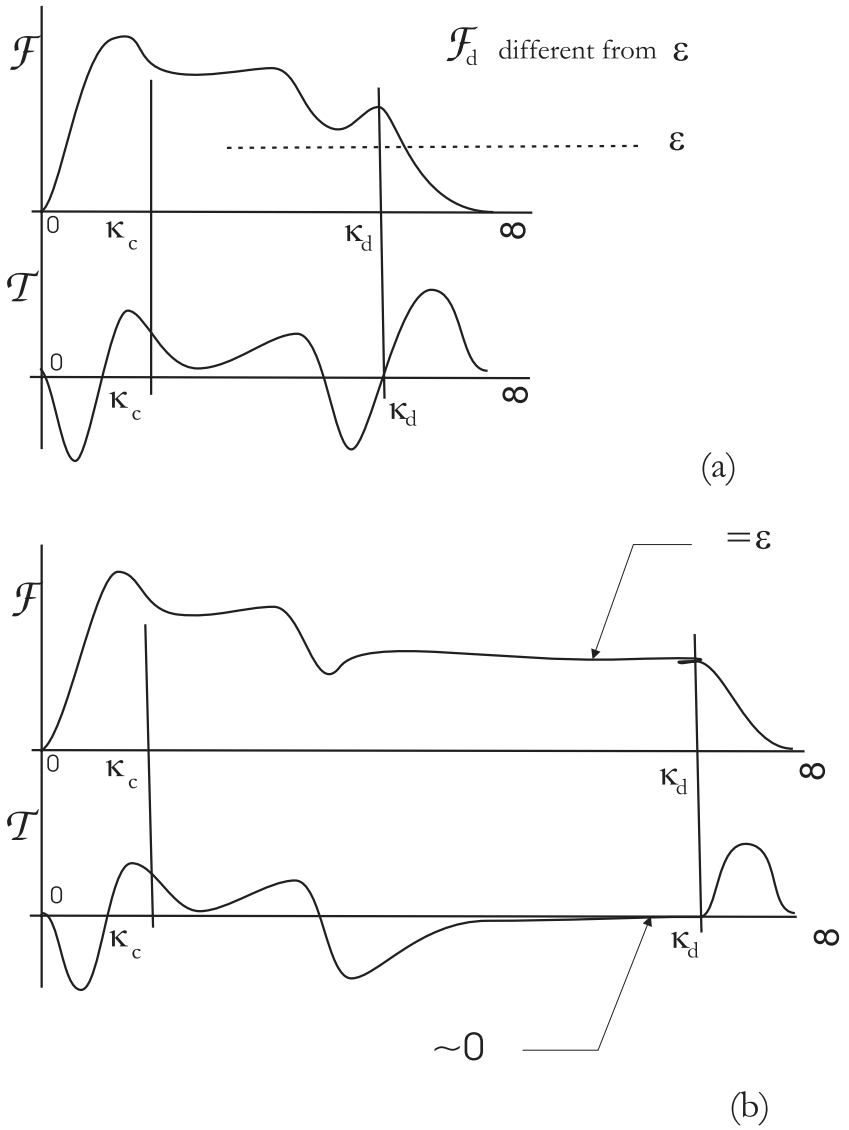

FIG. 3. Sketches of the spectral flux transfer $\mathcal{F}$ and spectral transfer term $\mathcal{T}$ with respect to the wave number κ in the spectral space for flows out of spectral equilibrium. (a) High Reynolds number; (b) infinite Reynolds number.

notice that the hypothesis consisting of increasing the turbulence Reynolds number (as long as an inertial cascade region already exists, i.e., if the Reynolds number is already sufficiently high) with the effect to lengthen the inertial zone without altering the statistical properties of the large eddies is implicitly contained in the PITM method. On the overall, because of its spectral foundation, the PITM method is mainly dedicated to the study of non-standard spectral distribution with some departures from the Kolmogorov distribution implying in most cases that $\mathcal{F}(\kappa_d) \neq F(\kappa_d)$.

D. Limiting behaviors

The subfilter models derived from the PITM method have the particularity to vary continuously with respect to the ratio of the turbulent length-scale to the grid-size L_e/Δ. Equation (58) indicates that the function $c_{sfs\epsilon_2}$ acts like a dynamic parameter which controls the part of the turbulence which is filtered relatively to the part which is explicitly calculated. In this method, the subfilter turbulence energy is interacting with the resolved energy, contrary to what appears for the Smagorinsky model. Regarding the two extreme limiting behaviors of the subfilter models, one can see that the models

behave like statistical RANS models when the parameter η_c goes to zero, whereas the computations switch to direct numerical simulation (DNS), provided the grid-size is sufficiently refined when η_c goes to ∞. In this latter case, the subfilter models are still running but become useless! Before switching to DNS, the subfilter models behave like the Smagorinsky model when the filter width is small corresponding to large values of the wave number κ_d but not infinite. This has been demonstrated by assuming a Kolmogorov law in the inertial zone and spectral equilibrium conditions in the vicinity of the wave number κ_d.[16]

V. TEST OF THE GENERIC DISSIPATION-RATE EQUATION ON A SELF-SIMILAR ANALYTICAL FLOW EXAMPLE

A. Objective

The objective of this section is to evaluate the coefficients c_{ϵ_2} and $c_{sfs\epsilon_2}$ when the dissipative wave number κ_d goes to infinity with the aim to demonstrate that these coefficients take on finite values. The demonstration is restricted to a particular example such as the case of the self-similar decay of homogeneous isotropic turbulence. The determination of the coefficient $c_{sfs\epsilon_2}$ defined in Eq. (37), first requires to compute the energy flux $F(\kappa_d, t)$ and the energy transfer $\mathcal{F}(\kappa_d, t)$ versus the time t of the turbulence decay. The present demonstration relies upon the generic dissipation-rate equation applied to a particular case assuming the Kovasznay transfer closure and self-similarity hypothesis. This flow has been studied by Reid and Harris[28,56] and provides a useful test case of reference. The method consists of solving in time and wave number the spectral equation written for homogeneous isotropic inviscid flows

$$\frac{\partial E(\kappa, t)}{\partial t} = -\frac{\partial \mathcal{F}(\kappa, t)}{\partial \kappa}. \tag{69}$$

B. The analytical solution of Reid and Harris

We consider similarity solutions given for the energy spectrum and transfer function in the initial period of decay of homogeneous isotropic turbulence for large values of the turbulent Reynolds numbers under self-similarity conditions.[28] The general self-preservation hypothesis implies that the energy spectrum can be written in the reduced form as follows:[57]

$$E(\kappa, t) = H(t)\, G(\gamma) = \frac{b}{\sqrt{t}}\, G(\kappa\sqrt{at}) = C_\kappa \epsilon^{2/3} \kappa^{-5/3}, \tag{70}$$

where H and G are similarity functions, $\gamma(t) = \kappa\sqrt{at}$ is a similarity variable whereas a and b denote constant coefficients. The new independent variables are now γ and t instead of κ and t. As a consequence of Eq. (70), $E(t) \propto t^{-1/2}$ if $\kappa(t) \propto t^{-1/2}$ implying that $\epsilon(t) \propto t^{-2}$ so that $d(\epsilon t^2) = 0$ or equivalently

$$\frac{\partial \epsilon}{\partial t} = -2\frac{\epsilon}{t}. \tag{71}$$

As an example, the decay law of the density spectrum is illustrated in Figure 4. In the absence of turbulent production, the equation $\partial k/\partial t = -\epsilon$ implies that $k(t) \propto t^{-1}$ and that the turbulence time scale $k/\epsilon = t$. Equation (69) can be solved by expanding the density spectrum $E(\kappa, t)$ as Taylor series of the dimensionless variable $z(\kappa, t) = \epsilon(t)^{-1/3}\kappa^{-2/3}t^{-1}$ where κ and t are independent variables and assuming the Kovasznay's hypothesis for the transfer term. As a result of the analytical calculation developed in Appendix B, one can obtain the Taylor series expansions for both the density spectrum $E(\kappa, t)$ and the transfer term $\mathcal{F}(\kappa, t)$ that read

$$E(\kappa, t) = C_\kappa \epsilon^{2/3}\kappa^{-5/3} - \frac{4}{3} {C_\kappa}^2 \epsilon^{1/3} \frac{\kappa^{-7/3}}{t} + \frac{2}{3} {C_\kappa}^3 \frac{\kappa^{-3}}{t^2} - \frac{8}{81} {C_\kappa}^4 \epsilon^{-1/3} \frac{\kappa^{-11/3}}{t^3} + \epsilon^{2/3}\kappa^{-5/3} O(z^4), \tag{72}$$

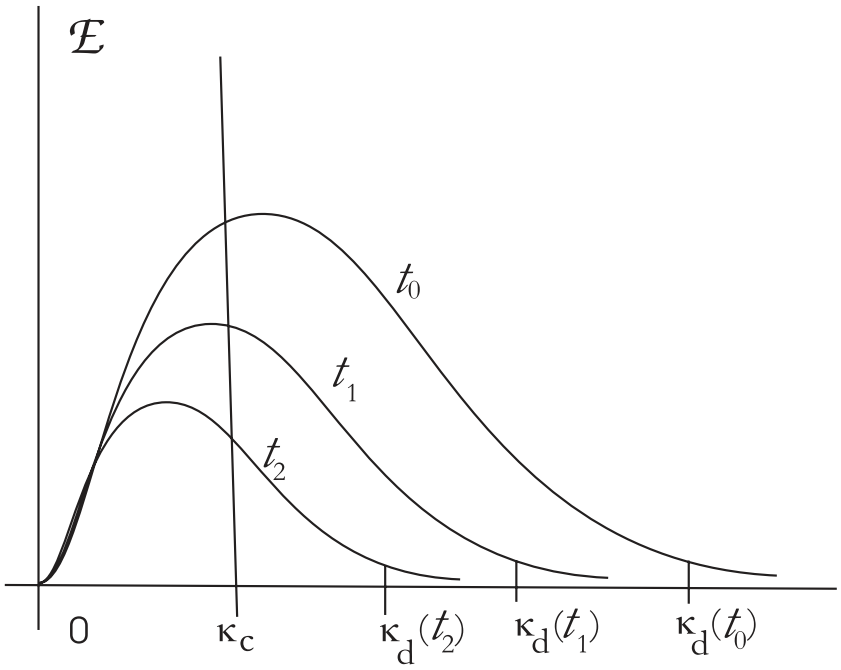

FIG. 4. Evolution of the density spectrum E given by Eq. (72) corresponding to the self-similar decay of turbulence.

and

$$\mathcal{F}(\kappa,t)=\epsilon-2C_\kappa\frac{\epsilon^{2/3}\kappa^{-2/3}}{t}+\frac{5}{3}{C_\kappa}^2\frac{\epsilon^{1/3}\kappa^{-4/3}}{t^2}-\frac{2}{3}{C_\kappa}^3\frac{\kappa^{-2}}{t^3}+\epsilon O(z^4). \tag{73}$$

These analytical results will form the basis of a test of the generic model for the ϵ equation. The coefficients of the generic dissipation-rate equation will be calculated in this particular case in order to verify that they both remain finite. Before, it is worth emphasizing again that the first term in the right-hand side of Eq. (73) which is the major transfer term contributes for nothing in Eq. (69). The active term is, in fact, the smaller second term in the right-hand side of Eq. (73) which represent the imbalance. The counterpart in the PITM method is the $(F-\mathcal{F})$ flux imbalance which appears as the acting mechanism. The imbalance in decaying isotropic turbulence has been shown in Bos *et al.*[58] to explain the difference between decaying and forced isotropic turbulence.

C. Consequences on the generic dissipation equation

1. Full statistical case where κ_c equals zero

We consider the full statistical case where κ_c equals zero. In this condition, the only splitting wave number is κ_d defined by $\kappa_d=\zeta_d\epsilon/k^{3/2}$. In the case of self-similar case, it is of interest to remark that $\epsilon/k^{3/2}=1/\sqrt{at}$ (see Appendix B) so that $\kappa_d=\zeta_d/\sqrt{at}$ and thus $\zeta_d=\kappa_d\sqrt{at}$. This relation shows that the coefficient ζ_d is nothing else than the similarity dimensionless variable $\gamma_d=\kappa_d\sqrt{at}$ introduced in Eq. (70) in this very special case. The question now is to compute the fluxes $F(\kappa_d,t)$ and $\mathcal{F}(\kappa_d,t)$ that appears in Eq. (39). In the PITM method, we usually assume that the partial turbulent energy associated to the spectral zone $[\kappa_d,\infty[$ at very high wave numbers is very weak and is currently considered as negligible leading to the well-known flux equation $F(\kappa_d,t)=\epsilon$. However, in the present analytical application, the Reid and Harris solution is indeed extending up to infinity turbulent Reynolds number and to be exact, one has to account for this energy through

the relation assuming the Kolmogorov law

$$\int_{\kappa_d}^{\infty} E(\kappa,t)\,d\kappa = \frac{3}{2}C_\kappa\,\epsilon^{2/3}\kappa_d^{-2/3}. \tag{74}$$

The energy transfer $F(\kappa_d,\ t)$ is obtained by means of the energy balance equation in the zone $[\kappa_d,\ \infty[$ as

$$F(\kappa_d,t) = \epsilon + \frac{\partial}{\partial t}\int_{\kappa_d}^{\infty} E(\kappa,t)\,d\kappa. \tag{75}$$

Using Eq. (32) for expressing the wave number κ_d with respect to ϵ and k, one can obtain

$$\int_{\kappa_d}^{\infty} E(\kappa,t)\,d\kappa = \frac{3}{2}C_\kappa\,\epsilon^{2/3}\left(\zeta_d\frac{\epsilon}{k^{3/2}}\right)^{-2/3} = \frac{3}{2}C_\kappa\,\zeta_d^{-2/3}\,k, \tag{76}$$

and its time derivative is obtained as

$$\frac{\partial}{\partial t}\int_{\kappa_d}^{\infty} E(\kappa,t)\,d\kappa = -\frac{3}{2}C_\kappa\,\zeta_d^{-2/3}\,\epsilon \tag{77}$$

leading to the result

$$F(\kappa_d,t) = \epsilon\left[1 - \frac{3}{2}C_\kappa\,\zeta_d^{-2/3}\right]. \tag{78}$$

Considering the first terms in the Taylor series (73) applied for the wave number κ_d

$$\mathcal{F}(\kappa_d,t) = \epsilon - 2C_\kappa\,\epsilon^{2/3}\frac{\kappa_d^{-2/3}}{t}, \tag{79}$$

and using Eq. (32) for expressing the wave number κ_d, taking into account that $k = \epsilon t$, then Eq. (79) reduces to

$$\mathcal{F}(\kappa_d,t) = \epsilon\left[1 - 2C_\kappa\,\zeta_d^{-2/3}\right]. \tag{80}$$

It is then easy to compute the flux difference $\mathcal{F}(\kappa_d,t) - F(\kappa_d,t) = -C_\kappa\,\zeta_d^{-2/3}\epsilon/2$ using Eqs. (78) and (80), respectively. Taking also into account that $\kappa_d E_d = C_\kappa\epsilon^{2/3}\kappa_d^{-2/3}$, one can find that the coefficient c_{ϵ_2} appearing in the dissipation-rate transport equation takes on a finite value

$$c_{\epsilon_2} = \frac{3}{2} - \frac{\langle k_{sfs}\rangle}{\kappa_d E(\kappa_d)}\left(\frac{\mathcal{F}(\kappa_d) - F(\kappa_d)}{\epsilon}\right) = 2. \tag{81}$$

The important fact is that the coefficient is indeed finite. The precise numerical value $c_{sfs\epsilon_2} = 2$ is not at all surprising since it comes from the self-preserving hypothesis (see also Appendix C) implying that

$$\frac{\partial\epsilon}{\partial t} = -c_{\epsilon_2}\frac{\epsilon^2}{k} = -2\frac{\epsilon^2}{k}. \tag{82}$$

2. Subfilter turbulence case where κ_c is non-zero

The partial energy in the wave number range $[\kappa_d,\ \infty[$ is now given by

$$\int_{\kappa_d}^{\infty} E(\kappa)\,d\kappa = \frac{3}{2}C_\kappa\,\zeta_c^{-2/3}\,\langle k_{sfs}\rangle\left(\frac{\kappa_d}{\kappa_d - \kappa_c}\right)^{-2/3}, \tag{83}$$

where in this equation, Eq. (30) has been used. Considering that $\kappa_d \gg \kappa_c$, the temporal derivative of Eq. (83) in a first approximation reads

$$\frac{\partial}{\partial t}\int_{\kappa_d}^{\infty} E(\kappa)\,d\kappa \approx \frac{3}{2}C_\kappa\,\zeta_c^{-2/3}\left(\frac{\kappa_d}{\kappa_d - \kappa_c}\right)^{-2/3}\frac{d\langle k_{sfs}\rangle}{dt}. \tag{84}$$

In order to get an acceptable approximation for the derivative $d\langle k_{sfs}\rangle/dt$, it is then necessary to account for the total shape of the spectrum, while the Reid and Harris solution only apply to the inertial zone. A continuity approximation satisfying $\langle k_{sfs}\rangle/k \to 1$ when $\kappa_c \to 0$ has to be provided. This is made by setting

$$\frac{\langle k_{sfs}\rangle}{k} = Q(\eta_c), \tag{85}$$

where Q denotes an analytical function of the dimensionless parameter $\eta_c = \kappa_c k^{3/2}/\epsilon$, yielding

$$\frac{d\langle k_{sfs}\rangle}{dt} = Q(\eta_c)\frac{dk}{dt} + k\frac{dQ(\eta_c)}{dt} = -\epsilon\, Q(\eta_c) + k\frac{dQ(\eta_c)}{d\eta_c}\frac{d\eta_c}{dt}. \tag{86}$$

The derivative $d\eta_c/dt$ in the case of the self-similar decay of homogeneous isotropic turbulence is given by

$$\frac{d\eta_c}{dt} = \frac{\kappa_c}{\epsilon^2}\left(\frac{3}{2}\epsilon k^{1/2}\frac{dk}{dt} - k^{3/2}\frac{d\epsilon}{dt}\right) = \frac{\kappa_c}{\epsilon^2}\left(-\frac{3}{2}k^{1/2}\epsilon^2 + 2k^{3/2}\frac{\epsilon^2}{k}\right) = \frac{1}{2}\kappa_c k^{1/2} \tag{87}$$

so that

$$\frac{dQ(\eta_c)}{dt} = -\epsilon\, Q(\eta_c) + \frac{1}{2}\kappa_c k^{3/2}\frac{dQ_{\eta_c}}{d\eta_c} \tag{88}$$

and finally

$$\frac{d\langle k_{sfs}\rangle}{dt} = -\epsilon\, Q(\eta_c)\left[1 - \frac{\eta_c}{2}\frac{d\ln Q(\eta_c)}{d\eta_c}\right]. \tag{89}$$

Hence, the energy flux $F(\kappa_d)$ defined such as in Eq. (75) can be computed using Eqs. (84) and (89) leading to

$$F(\kappa_d, t) = \epsilon\left[1 - \frac{3}{2}C_\kappa\,\zeta_c^{-2/3}\left(\frac{\kappa_d}{\kappa_d - \kappa_c}\right)^{-2/3}\frac{\langle k_{sfs}\rangle}{k}\left(1 - \frac{\eta_c}{2}\frac{d\ln Q(\eta_c)}{d\eta_c}\right)\right]. \tag{90}$$

From the Taylor series (73) using the similarity relation $\epsilon^{-1/3}/t = \epsilon^{2/3}/k$, one also gets

$$\mathcal{F}(\kappa_d, t) = \epsilon\left[1 - 2C_\kappa\,\zeta_c^{-2/3}\left(\frac{\kappa_d}{\kappa_d - \kappa_c}\right)^{-2/3}\frac{\langle k_{sfs}\rangle}{k}\right]. \tag{91}$$

The difference between Eqs. (90) and (91) is then

$$\mathcal{F}(\kappa_d, t) - F(\kappa_d, t) = -\frac{C_\kappa}{2}\,\zeta_c^{-2/3}\left(\frac{\kappa_d}{\kappa_d - \kappa_c}\right)^{-2/3}\frac{\langle k_{sfs}\rangle}{k}\left[1 + \frac{3}{2}\eta_c\frac{d\ln Q(\eta_c)}{d\eta_c}\right] \tag{92}$$

leading to the final result for the $c_{sfs\epsilon_2}$ coefficient appearing in Eq. (37)

$$c_{sfs\epsilon_2} = \frac{3}{2} + \frac{1}{2}\frac{\langle k_{sfs}\rangle}{k}\left[1 + \frac{3}{2}\eta_c\frac{d\ln Q(\eta_c)}{d\eta_c}\right]. \tag{93}$$

Equation (93) written in a compact form can be applied whatever the function $Q = \langle k_{sfs}\rangle/k$ introduced in the analytical development. For the particular choice of the Von Kármán type spectrum defined in Eq. (56) and corresponding to

$$Q = \frac{\langle k_{sfs}\rangle}{k} = (1 + \beta_\eta\eta_c^3)^{-2/9}, \tag{94}$$

it is straightforward to get

$$\frac{d\ln Q(\eta_c)}{d\eta_c} = -\frac{2}{3}\frac{\beta_\eta\eta_c^2}{(1 + \beta_\eta\eta_c^3)} \tag{95}$$

leading to the final result

$$c_{sfs\epsilon_2} = \frac{3}{2} + \frac{1}{2}\frac{\langle k_{sfs}\rangle}{k}\left[1 - \frac{\beta_\eta\eta_c^3}{1 + \beta_\eta\eta_c^3}\right]. \tag{96}$$

When $\eta_c \to \infty$, the limit $c_{sfs\epsilon_2} \to 3/2$ is obtained, suggesting that the turbulence in the $[\kappa_c, \kappa_d]$ slice is vanishing (see Appendix A) leading to a DNS like simulation. As an interesting

result, one can see that $c_{sfs\epsilon_2}$ always takes on a finite value whatever the domain variation of κ_d and in particular when κ_d goes to ∞. On the other hand, one can remark that $\lim_{\eta_c \to 0} c_{sfs\epsilon_2}(\eta_c) = 2$ according to the previous result found in full statistical modeling where $\kappa_c = 0$. We have thus shown that in a particular analytical case, taken as a test example, the coefficients of the dissipation-rate equation remain finite when κ_d goes to infinity, even if the generic form of $c_{sfs\epsilon_2}$ coefficient takes the indeterminate form 0/0 at infinity. Of course, the $c_{sfs\epsilon_2}$ value thus obtained is by no means universal but would take on a different numerical value in other particular examples.

As a marginal remark, one can see that Eq. (89) provides the temporal evolution of the subfilter energy

$$\frac{\partial \langle k_{sfs} \rangle}{\partial t} = -\epsilon\, Q(\eta_c) \frac{1 + \frac{4}{3}\beta_\eta \eta^3}{1 + \beta_\eta \eta^3}. \tag{97}$$

Equation (97) indicates that the decay of the subfilter energy is governed by the parameter η varying from 0 to ∞. In particular, when $\eta_c \to 0$, Eq. (97) leads to equation

$$\frac{\partial \langle k_{sfs} \rangle}{\partial t} = -\epsilon\, Q(\eta_c) = \frac{\langle k_{sfs} \rangle}{k} \frac{\partial k}{\partial t}, \tag{98}$$

which is the same as Eq. (52) introduced in Sec. IV A whereas when $\eta_c \to \infty$

$$\frac{\partial \langle k_{sfs} \rangle}{\partial t} = -\frac{4}{3}\epsilon\, Q(\eta_c) = \frac{4}{3} \frac{\langle k_{sfs} \rangle}{k} \frac{\partial k}{\partial t} \tag{99}$$

meaning that the decay is increased relatively to the ratio $\langle k_{sfs} \rangle / k$. This result is found to be in agreement with the physics of turbulence suggesting that the small scales decrease more rapidly than the large scales energy.

VI. THE PITM METHOD IN PRACTICE

The PITM method is based on the system of the instantaneous transport equations for the subfilter energy (29), the subfilter scale stresses (28), and the subfilter dissipation-rate inspired from Eq. (55) that reads

$$\frac{D\epsilon_{sfs}}{Dt} = c_{sfs\epsilon_1} \frac{\epsilon_{sfs}}{k_{sfs}} P_{sfs} - c_{sfs\epsilon_2} \frac{\epsilon_{sfs}^2}{k_{sfs}} + (J_\epsilon)_{sfs}, \tag{100}$$

where in this equation, the diffusion term $(J_\epsilon)_{sfs}$ has been embedded for handling non-homogeneous flows. In Eq. (100), the $c_{sfs\epsilon_1}$ coefficient is equal to the corresponding coefficient in the companion statistical model $c_{sfs\epsilon_1} = c_{\epsilon_1}$ whereas $c_{sfs\epsilon_2}$ is the dynamic coefficient computed by means of Eq. (58).

A. Subfilter scale viscosity models

The subfilter scale viscosity models are transposed from RANS $k - \epsilon$ models initially developed by Jones and Launder,[59] and Launder and Sharma.[60] These subfilter models derived from the PITM method rely on Eqs. (29) and (100) where the different terms appearing in these equations are modeled using an eddy viscosity hypothesis ν_{sfs} defined itself by[12]

$$\nu_{sfs} = c_\mu \frac{k_{sfs}^2}{\epsilon_{sfs}}, \tag{101}$$

where c_μ is a constant coefficient. In this case, the subfilter turbulent stresses are proportional to the filtered deformation of the flow field

$$(\tau_{ij})_{sfs} = -\nu_{sfs} \left(\frac{\partial u_i}{\partial x_j} + \frac{\partial u_j}{\partial x_i} \right) + \frac{2}{3} k_{sfs} \delta_{ij}. \tag{102}$$

The production term P_{sfs} due to the interaction between the subfilter stress and the filtered gradient velocity is

$$P_{sfs} = -(\tau_{ij})_{sfs} \frac{\partial \bar{u}_j}{\partial x_i}. \tag{103}$$

The diffusion term J_{sfs} appearing in Eq. (29) is modeled by a gradient law hypothesis

$$J_{sfs} = \frac{\partial}{\partial x_j}\left[\left(\nu + \frac{\nu_{sfs}}{\sigma_k}\right)\frac{\partial k_{sfs}}{\partial x_j}\right], \tag{104}$$

where σ_k is a constant coefficient. In the same way, the diffusion term $(J_\epsilon)_{sfs}$ appearing in Eq. (100) is modeled as

$$(J_\epsilon)_{sfs} = \frac{\partial}{\partial x_j}\left[\left(\nu + \frac{\nu_{sfs}}{\sigma_\epsilon}\right)\frac{\partial \epsilon_{sfs}}{\partial x_j}\right], \tag{105}$$

where σ_ϵ is a constant coefficient. Recently, more advanced viscosity subfilter models based on the PITM method have emerged. One is the $k_{sfs} - \epsilon_{sfs} - \zeta - f$ model[25] where ζ represents the ratio of the normal velocity to the turbulent energy and f is an elliptic function inspired from the Durbin RANS model[61] taking into account the Speziale-Sarkar-Gatski (SSG) model.[62] The second one is the $k_{sfs} - \omega_{sfs}$ subfilter model inspired from the RANS $k - \omega$ SST model.[63]

B. Subfilter scale stress models

The subfilter scale stress models are transposed from RANS-RSM turbulence models initially developed by Launder *et al.*[20] and Speziale *et al.*[62] at high Reynolds numbers. These subfilter models derived from the PITM method are based on Eqs. (28) and (100). In the contrary to the two-equation subfilter model which requires to model the production term P_{sfs}, the production term $(P_{ij})_{sfs}$ appearing in the subfilter-scale stress model takes the exact expression

$$(P_{ij})_{sfs} = -(\tau_{ik})_{sfs}\frac{\partial \bar{u}_j}{\partial x_k} - (\tau_{jk})_{sfs}\frac{\partial \bar{u}_i}{\partial x_k}. \tag{106}$$

However, the redistribution, diffusion and dissipation terms need to be modeled. Like in RANS modeling, the redistribution term $(\Psi_{ij})_{sfs}$ is decomposed into a slow part $(\Psi^1_{ij})_{sfs}$ which characterizes the return to isotropy due to the action of turbulence on itself and a rapid part $(\Psi^2_{ij})_{sfs}$ which describes the return to isotropy by action of the filtered velocity gradient. The term $(\Psi^1_{ij})_{sfs}$ is modeled on the one hand assuming that the usual statistical Reynolds stress models must be recovered in the limit of vanishing cutoff wave number κ_c and on the other hand considering also that the small scales return more rapidly to isotropy than the large scales before cascading into smaller scales by nonlinear interactions

$$(\Psi^1_{ij})_{sfs} = -c_1\, c_{sfs_1}\frac{\epsilon_{sfs}}{k_{sfs}}\left((\tau_{ij})_{sfs} - \frac{2}{3}k_{sfs}\,\delta_{ij}\right). \tag{107}$$

In Eq. (107), c_1 is the usual Rotta coefficient used in statistical RANS modeling whereas c_{sfs_1} is an increasing function of the parameter η_c empirically calibrated as

$$c_{sfs_1}(\eta_c) = \frac{1 + \alpha_{\eta 1}\,\eta_c^2}{1 + \alpha_{\eta 2}\,\eta_c^2}, \tag{108}$$

where $\alpha_{\eta 1}, \alpha_{\eta 2}$ are constant coefficients verifying the condition $\alpha_{\eta 1} > \alpha_{\eta 2}$. The second term $(\Psi^2_{ij})_{sfs}$ is modeled by means of the rapid distortion theory for homogeneous strained turbulence in an initially isotropic state[64]

$$(\Psi^2_{ij})_{sfs} = -c_2\left((P_{ij})_{sfs} - \frac{1}{3}(P_{mm})_{sfs}\,\delta_{ij}\right), \tag{109}$$

where the coefficient c_2 remains the same as in statistical modeling. The diffusion term $(J_{ij})_{sfs}$ appearing in Eq. (28) associated to the fluctuating velocities and pressure together with the molecular

diffusion is modeled assuming a gradient law hypothesis

$$(J_{ij})_{sfs} = \frac{\partial}{\partial x_k}\left(\nu\frac{\partial(\tau_{ij})_{sfs}}{\partial x_k} + c_s\frac{k_{sfs}}{\epsilon_{sfs}}(\tau_{kl})_{sfs}\frac{\partial(\tau_{ij})_{sfs}}{\partial x_l}\right), \tag{110}$$

where c_s is a constant numerical coefficient. In the case of the flux equation, the diffusion term $(J_\epsilon)_{sfs}$ appearing in the subfilter dissipation-rate equation (100) is modeled assuming a well-known gradient law hypothesis referring to the tensorial eddy viscosity concept as follows:

$$(J_\epsilon)_{sfs} = \frac{\partial}{\partial x_j}\left(\nu\frac{\partial\epsilon_{sfs}}{\partial x_j} + c_\epsilon\frac{k_{sfs}}{\epsilon_{sfs}}(\tau_{jm})_{sfs}\frac{\partial\epsilon_{sfs}}{\partial x_m}\right), \tag{111}$$

where the coefficient c_ϵ remains constant. The coefficients used in these energy and stress subfilter models can be found in the original papers.[12,15] Other authors, Fadai-Ghotbi *et al.*[18,19] have recently developed another subfilter-scale stress model derived from the temporal partially integrated transport modeling method.[18] Their model is inspired from the RANS-RSM model developed by Manceau and Hanjalic[23] and it is based itself on the Durbin elliptic blending approach[61] taking into account the SSG model.[62]

C. Relaxation mechanism and convergence acceleration

The key equation for the PITM method is Eq. (54) that in terms of the grid spacing becomes Eq. (62). The ratio of the grid spacing (more precisely the filter width) to the turbulence macroscale (scale of the total turbulent field including subfilter and resolved scales) is the key parameter that determines the equilibrium value of the ratio between the modeled and the total kinetic turbulent energy (62). The coefficient $c_{sfs\epsilon_2}$ defined in Eq. (58) indeed controls the amount of energy which is modeled relatively to the amount which is simulated. For equilibrium flows, it is observed that the ratio of the subfilter energy to the total energy computed by the simulation $r_{CFD} = \langle k_{sfs}\rangle/k$ is close to the equilibrium value $r_{eq} = (\langle k_{sfs}\rangle/k)_{eq}$ solution of Eq. (57) deduced from the theoretical Von Kármán energy spectrum $E(\kappa)$, once the permanent state is reached after a long CPU time. In strongly non-equilibrium flows, there is a time lag. The use of r_{eq} in Eq. (62) allows to relate directly the turbulence energy ratio to the ratio of the turbulence to grid length scales. As mentioned earlier, the mechanism acting in the ϵ equation can be interpreted as a "return to equilibrium" process. How this targeted value is related in practical computations to the observed values can be evidenced as a relaxation process on the usual dissipation rate equation. Considering, to remain simple, the case of homogeneous turbulence at large Reynolds numbers ($\langle\epsilon_{sfs}\rangle = \epsilon$ since $\langle\epsilon^<\rangle \approx 0$), the subfilter scale equations for energy (29) and transfer (55) can be written as

$$\frac{\partial\epsilon}{\partial t} = c_{\epsilon_1}\frac{\epsilon\langle P_{sfs}\rangle}{\langle k_{sfs}\rangle} - c_{sfs\epsilon_2}\frac{\epsilon^2}{\langle k_{sfs}\rangle}, \tag{112}$$

coupled with the equation

$$\frac{\partial\langle k_{sfs}\rangle}{\partial t} = \langle P_{sfs}\rangle - \epsilon. \tag{113}$$

Equation (58) expresses in fact the relation with the equilibrium turbulence energy ratio

$$c_{sfs\epsilon_2} = c_{\epsilon_1} + (c_{\epsilon_2} - c_{\epsilon_1})\left(\frac{\langle k_{sfs}\rangle}{k}\right)_{eq}. \tag{114}$$

In order to get an intuitive understanding of how the relaxation works, let us suppose that the evolution of the turbulence field is approximately self-similar so that taking into account the total turbulence energy equation

$$\frac{\partial k}{\partial t} = P - \epsilon \tag{115}$$

together with Eq. (113), one gets

$$\frac{\langle k_{sfs}\rangle}{k} = \frac{\langle P_{sfs}\rangle - \epsilon}{P - \epsilon}, \tag{116}$$

which is the same as Eq. (52) written for $\langle\epsilon_{sfs}\rangle = \epsilon$. Note that this approximation is just used for the present simplified demonstration but not in the model itself. Using then Eq. (116) to eliminate $\langle P_{sfs}\rangle$

appearing in Eq. (112) in conjunction with the basic Eq. (114) derived from the PITM method, gives after some straightforward algebra the resulting equation

$$\frac{\partial \epsilon}{\partial t} = c_{\epsilon_1}\frac{\epsilon\langle P\rangle}{k} - c_{\epsilon_2}\frac{\epsilon^2}{k} + (c_{\epsilon_2} - c_{\epsilon_1})\frac{\epsilon^2}{\langle k_{sfs}\rangle}\left[\frac{\langle k_{sfs}\rangle}{k} - \left(\frac{\langle k_{sfs}\rangle}{k}\right)_{eq}\right]. \tag{117}$$

Comparing to the usual dissipation equation in statistical models, an extra term in bracket in the right-hand side of this equation now appears that acts as a relaxation term towards the equilibrium or *target value*. More precisely, if $r_{CFD} = \langle k_{sfs}\rangle/k <$ equilibrium value r_{eq} (respectively, $>$ equilibrium value), then $\partial\epsilon/\partial t$ decreases (respectively, increases) and $r_{CFD} = \langle k_{sfs}\rangle/k$ increases (respectively, decreases) so that at the end of the iterative process, r_{CFD} approaches r_{eq} although the strict equality is not absolutely guaranteed if the flow remains out of spectral equilibrium.

In practice, for accelerating the numerical convergence towards the solution in the permanent state and to avoid the model to wander towards a purely RANS or LES limiting behavior during the transition phase, a procedure[19] is activated during the computations to force the model to approach more rapidly the expected energy ratio. The mechanism described before based upon physical considerations is then reinforced. To do that, the equilibrium energy ratio $r_{eq} = (\langle k_{sfs}\rangle/k)_{eq}$ given by Eq. (57) is then compared with the ratio value r_{CFD} computed by the simulation. The dynamic correction applied to the subfilter coefficient $\delta c_{sfs\epsilon_2}$ is then calculated by means of the parameter r_{CFD}/r_{eq} as follows:[17,19]

$$\delta c_{sfs\epsilon_2} = \chi\, c_{sfs\epsilon_2}\left(1 - \frac{r_{CFD}}{r_{eq}}\right), \tag{118}$$

where χ is a constant parameter set to 0.1 once for all.

D. Extensions

The most important outgrowth of the subfilter models is their extensions to low Reynolds number turbulence, a feature which is absolutely necessary to deal with real turbulent flows and in particular wall flows. In low Reynolds number turbulence, the subfilter models need to be modified in two main aspects. The first aspect concerns the evaluation of the dissipation-rate. Indeed, as the inertial zone shortens and can even disappear completely, the dissipation process can occur in the resolved part of the flow so that it is necessary to account for the resolved part of the viscous dissipation. In order to take into account all contributions, the true dissipation rate ϵ becomes the sum of the modeled dissipation-rate $\langle\epsilon_{sfs}\rangle$ and the resolved dissipation $\epsilon^<$ as

$$\epsilon = \langle\epsilon_{sfs}\rangle + \epsilon^<, \tag{119}$$

where $\epsilon^<$ is defined in Eq. (60). In low Reynolds number turbulence, this is the total dissipation-rate that has to be used in Eq. (59). The conditions under which this term may be important can be determined approximately using turbulence scales. As usually assumed, if one considers that an appreciable viscous dissipation occurs for scales smaller than the Taylor microscale $\lambda = \sqrt{15\nu k/\epsilon}$, the condition to satisfy takes the form

$$\kappa_c > \frac{1}{\lambda} \text{ or equivalently } \eta_c = \kappa_c L_e > \sqrt{\frac{Re_T}{15}} \tag{120}$$

with $Re_T = L_e\sqrt{k}/\nu = k^2/(\nu\epsilon)$ is the turbulent Reynolds number. At the extreme limit, if $\kappa_c = 1/\eta_K$ with $\eta_K = (\nu^3/\epsilon)^{1/4}$ being the Kolmogorov scale, or equivalently $\eta_c = Re_T^{3/4}$, then the simulation would become a DNS. So, in the presence of resolved dissipation, the input energy flux entering the subfilter zone though the wave number κ_c will be reduced of the corresponding same amount, but there is no reason to think that the form of the dissipation-rate equation should be modified. For illustrative purposes, Figure 5 has been worked out to show the energy density spectrum, productive, transfer, and dissipative zones as well as the energy flux acting in the spectral space at low Reynolds number. The second aspect concerns the coefficients used in the models. Like in statistical modeling, the model coefficients must become some functions of the local turbulence

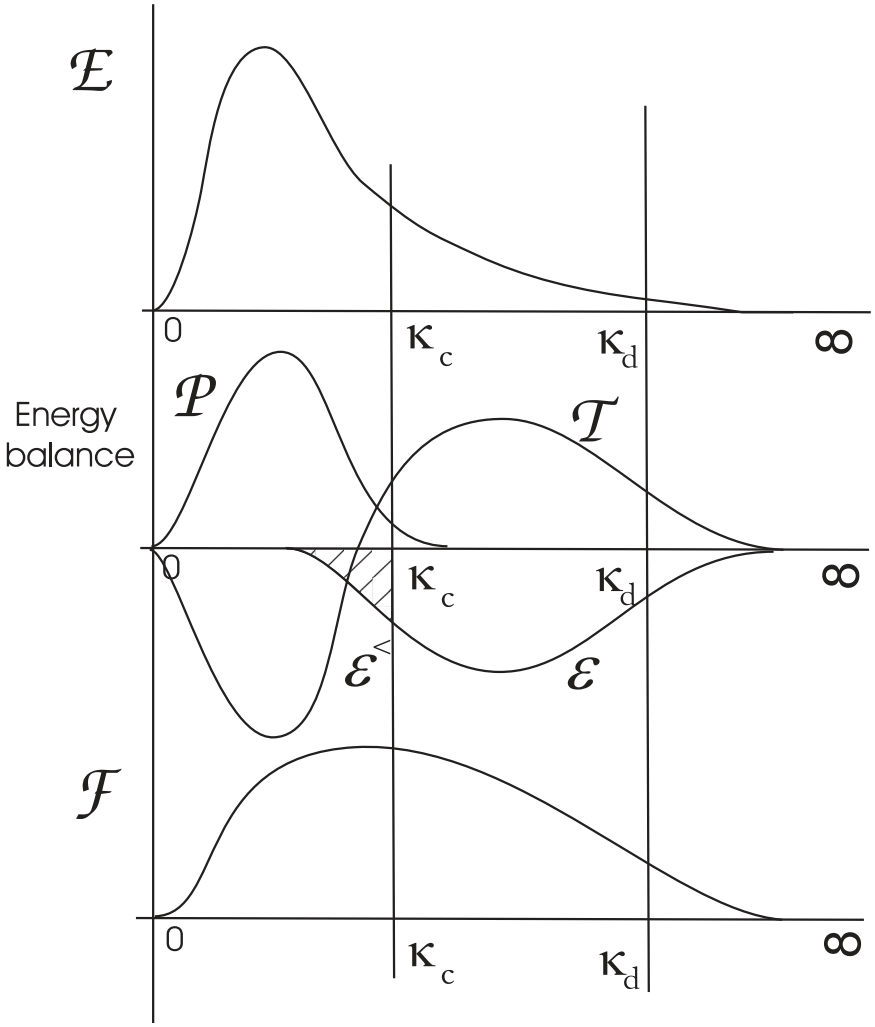

FIG. 5. Sketches of the density energy spectrum E, spectral flux transfer $\mathcal{F}$, and spectral transfer term $\mathcal{T}$ with respect to the wave number κ in the spectral space at low Reynolds number.

Reynolds number and/or the turbulent invariants involving the anisotropy tensors for approaching wall regions. These functions are largely empirical and in the present case, they will be directly inspired from the statistical model counterparts. The practical formulation of the low Reynolds number counterparts of both viscosity and stress transport models are given in Refs. 12, 13, 17, and 19 using low Reynolds number corrections[21,60] or the elliptic blending approach.[23,61] Another promising extension of the approach is the extension to models accounting for directional dependence allowing a refined modeling of anisotropy. These models as initiated in Refs. 47, 65, 46, and 66 in statistical RANS closures include transport equations for the directional anisotropy in addition to the turbulent stresses. There is no doubt that this approach could be fruitfully extended to the PITM method in the near future.[67]

VII. SOME PITM SIMULATIONS EXAMPLES

As mentioned earlier, the PITM method can be applied to almost any usual statistical closure to convert it into an hybrid continuous model, for energy model as well as stress transport model. Most of the PITM applications achieved at present time does use subfilter scale stress transport equations.

A. PITM challenges

The PITM method has been especially developed for performing continuous hybrid non-zonal RANS-LES simulations of free and wall-bounded flows on coarse grids with a sufficient representativeness for engineering applications. This method is mainly dedicated to applications in non-equilibrium turbulence. The subfilter models derived from the PITM method are applied on the whole computational domain without arbitrary setting RANS or LES regions. In that sense, the turbulent models are able to automatically adapt themselves to the level of turbulence modeling required for the simulations. As shown in the preceding sections, the dimensionless parameter η involving both the grid spacing of the mesh and the turbulence length scale is the key parameter in the PITM method. The models are applied in their low Reynolds number versions for accurately reproducing the wall boundary layers of turbulent confined flows, the grid being sufficiently refined in the normal direction to the wall. This allows to avoid the requirement of empirical wall functions. In practice, the subfilter models derived from the PITM method behave like RANS models near the wall regions and more or less like LES in the core flows, with a progressive change. Among these subfilter models, the subfilter scale stress models are particularly recommended for simulating wall bounded flows because of the redistribution term that allows to reproduce the near wall flow anisotropy. In the following, we briefly mention some flow illustrations to get an insight into the PITM method in its capabilities to simulate unsteady flows, the physical analysis of these flows being extensively conducted in previous references. From a numerical point of view, the governing equations are integrated by a Runge-Kutta scheme of fourth-order accuracy in time whereas the convective fluxes are computed by a quasi-centered numerical scheme of second or fourth-order accuracy in space,[68] the space-time scheme combination being well appropriate for LES.

B. Simulation of homogeneous turbulence

The decay of homogeneous isotropic turbulence referring to the experiment of Comte-Bellot and Corrsin[69] has been simulated on a coarse grid[16] with a cutoff wave number κ_c defined such as the initial ratio of the subfilter energy to the total energy was roughly 1/3. Then, initial perturbed spectra with a peak or a defect of energy was considered for analyzing the model capabilities in strong non-equilibrium flow situations. As a result, it has been found that the PITM simulations reproduced very well the experimental data associated to the decay of the spectrum[69] and provided results in good qualitative agreement with EDQNM simulations.[35]

C. Simulation of non-homogeneous turbulence

Different bounded flows have been performed on coarse grids including the basic test case of fully turbulent channel flow[12,13,19] and more complex flows such as the channel flow with mass injection subjected to the development of natural unsteadiness,[13] the pulsed channel flow influenced by forced unsteadiness,[12] the channel flow over periodic hills[15,25,27] governed by interacting turbulence mechanisms associated with separation, recirculation and reattachment, and the channel flow subjected to a spanwise rotation ranging from moderate to higher rotation rates.[17] The prediction of rotating turbulent flows is known for the difficulty in modeling the subtle effects of the Coriolis forces. In particular, in the channel flow subjected to a spanwise rotation, any viscosity model is blind to rotation effects and misses completely the asymmetry character (stable and unstable sides) of the flow. This is why, the calculation in Ref. 17 makes use of a subfilter model including all the stress transport equations. This level of closure allows to account for explicit Coriolis effects in the stress equations to get satisfactory results because the Coriolis forces are naturally embodied in the equation, both in the source and redistribution terms. It is true, however, that implicit Coriolis effects also exist, that are not taken into account in the equations here, but they probably become important at very high rotational Reynolds numbers like for flows in inter-disk systems.[36] But such an account would be only possible through directional anisotropy sensitized models like in Refs. 36 and 67. Free turbulent flows were also simulated such as the turbulent spectral non-equilibrium flow created

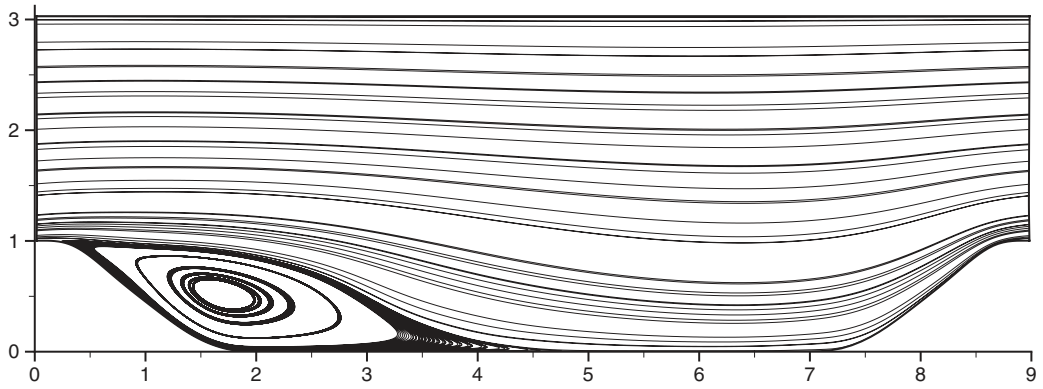

FIG. 6. Mean streamlines of the average flow field computed at the Reynolds number Re = 37 000. PITM simulation (160 × 60 × 100).

by the mixing of two turbulence fields of different scales in a shearless mixing layer.[70] As a result, it was found that the PITM method was able to simulate these turbulent flows on coarse grids with satisfactory agreement with the reference data and provided some details of the large flow structures, from a qualitative point of view.

D. Study of the coefficient $c_{sfs\epsilon_2}$ through one chosen example

As an example, we consider the calculation of turbulent flows over periodic hills at the high Reynolds number Re = 37 000 (Ref. 71) performed using the PITM method on a curvilinear grid 160 × 60 × 100 (≈1 × 10^6 grid points) in the streamwise, spanwise, and normal directions (x_1, x_2, x_3). The objective here being to study the coefficient $c_{sfs\epsilon_2}$ and not the flow in itself (see Refs. 15 and 25), only some characteristics of the flow and its turbulence properties will be briefly recalled in the following. Concerning the geometry, the hills constrict the channel by about one third of its height h and they are spaced at a distance of about 9 hills. Figure 6 shows the streamlines of the averaged flow field illustrating the recirculation zone as well as the turbulence effects associated with separation, recirculation, and flow reattachment of the boundary layer. At a first sight, one can see that the recirculation zone computed at Re = 37 000 is smaller than the one computed at the lower Reynolds number at Re = 10 595 plotted in Ref. 15. Figure 7 displays the evolutions of the dimensionless parameter $\eta_c = \kappa_c L_e$ in the cross section of the channel at the stations prior to the reattachment $x_1/h = 2$ and at the flow recovery station $x_1/h = 6$. This figure reveals that the parameter η_c goes to zero near the wall regions and reaches maximum values in the shear layer region. The high η_c values found in the present case can be explained by the relatively large value of the Reynolds number considering also that the core flow is dominated by unsteady large energy carrying scales which develop in the channel from the windward side of the first hill to the second hill. This remark suggests that, considering the particular discretization mesh chosen in the calculation, the PITM method behaves like a LES in the shear layer region where $x_3/h \approx 1$ and more or less like a RANS model in the wall regions $x_3/h \approx 0$ and $x_3/h \approx 3$. When comparing these evolutions at these two locations, it can be shown also that the parameter η_c takes on higher values at the station $x_1/h = 2$ than at the station $x_1/h = 6$. Physically, this outcome means that the PITM simulation resolves more large scales in the middle of the recirculation zone close to the leeward hill face than on the region of the windward slope of the hill. The main result is shown in Figure 8 which describes the evolutions of the coefficient $c_{sfs\epsilon_2}$ in the normal direction from the walls at the stations $x_1/h = 2$ and $x_1/h = 6$. As expected, these coefficient values stay nicely in scale between the two limiting statistical values $c_{\epsilon_1} = 1.50$ and $c_{\epsilon_2} = 1.90$ according to Eq. (54). The function $c_{sfs\epsilon_2}$ goes to the upper limit c_{ϵ_2} near the walls because of the parameter η_c involved in Eq. (58) is going to zero in that region, and then gradually decreases when moving away from the walls as the parameter η_c increases. As shown in the preceding sections, this result confirms that the PITM method varies continuously from

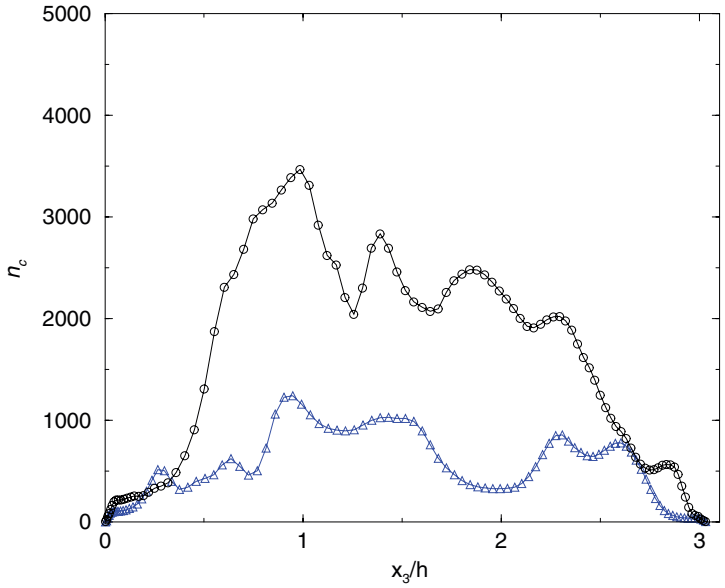

FIG. 7. Evolution of the parameter $\eta_c = \kappa_c L_e$ in different cross sections of the channel. (a) $x_1/h = 2$, ○: η_c; (b) $x_1/h = 6$, Δ: η_c.

quasi-URANS modeling in the wall region (although the grid is very refined $\Delta_3^+ = 0.5$) to large eddy simulations far away from the walls, with seamless coupling between these two regions. We emphasize again that this example is particular to flow under consideration and the discretization mesh which in the present case, determines the filter width. One can remark also, that it is always permissible to use a filter width larger than the mesh step, for numerical accuracy reasons, but it is often useless in practice.

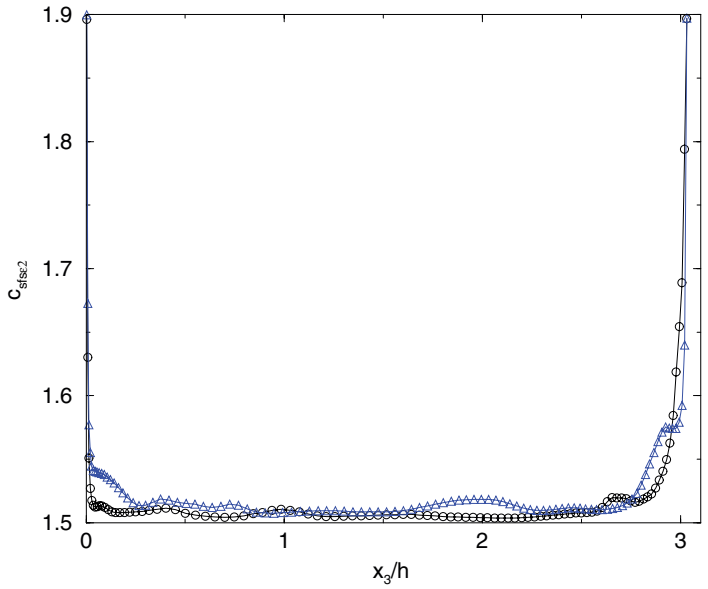

FIG. 8. Evolution of the $c_{sfs\epsilon_2}$ coefficient in different cross sections of the channel. (a) $x_1/h = 2$, ○: $c_{sfs\epsilon_2}$; (b) $x_1/h = 6$, Δ: $c_{sfs\epsilon_2}$.

VIII. CONCLUSION

In this work, we have first recalled the main building steps of the PITM method and we have given further insight into the physical mechanisms of the modeled equations. The underlying hypothesis of the PITM method have been thoroughly examined from a physical standpoint. A special attention has been devoted to the generic character of the subfilter dissipation-rate transport equation. In particular, we have demonstrated that it is possible to apply the PITM method to all statistical models with the aim to derive their corresponding subfilter models used in LES, provided some approximations are, however, conceded. Then, as an example, we have considered the self-similar analytical flow of Reid and Harris[28] obtained in the present case by means of Taylor series expansions taking into account the Kovasznay hypothesis for evaluating the transfer term. We have analytically calculated the functional coefficients c_{ϵ_2} and $c_{sfs\epsilon_2}$ used in RANS and LES methodologies, respectively, and we have proved that they both take on finite values in all cases. Finally, some flow illustrations were briefly mentioned to get a real appraisal of the PITM method in its capabilities to simulate unsteady flows on relatively coarse grids with a sufficient accuracy for engineering computations and the coefficient $c_{sfs\epsilon_2}$ was analyzed through one chosen example.

APPENDIX A: ON THE PHYSICAL MEANING OF $c_{sfs\epsilon_2}$ IN THE SPECTRAL SPACE

It is worth mentioning some consequences of the Kovasznay hypothesis in spectral space in connection with the flux equations used in multiple scale models. Let us consider the Kovasznay hypothesis for the transfer term,

$$\mathcal{F}(\kappa, t) = C_\kappa^{-3/2}\, E(\kappa, t)^{3/2}\, \kappa^{5/2}, \tag{A1}$$

and take the logarithmic partial time derivative of both sides, giving

$$\frac{1}{\mathcal{F}}\frac{\partial \mathcal{F}(\kappa, t)}{\partial t} = \frac{3}{2}\frac{1}{E}\frac{\partial E(\kappa, t)}{\partial t} \tag{A2}$$

taking into account the spectral energy equation in the inertial zone

$$\frac{\partial E(\kappa, t)}{\partial t} = -\frac{\partial \mathcal{F}(\kappa, t)}{\partial \kappa}, \tag{A3}$$

the previous equation becomes

$$\frac{\partial \mathcal{F}(\kappa, t)}{\partial t} = -\frac{3}{2}\frac{\mathcal{F}}{E}\frac{\partial \mathcal{F}(\kappa, t)}{\partial \kappa}. \tag{A4}$$

It is straightforward to discretize this latter equation using simple finite differences in the wave number space

$$\frac{\partial \mathcal{F}^{(m)}}{\partial t} = \frac{3}{2}\frac{\mathcal{F}^{(m)}}{E^{(m)}}\frac{\mathcal{F}^{(m-1)} - \mathcal{F}^{(m)}}{\Delta\kappa}. \tag{A5}$$

The term $E^{(m)}\Delta\kappa$ is in fact the partial turbulent energy $k^{(m)}$ comprised within the spectral slice $[\kappa_{m-1}, \kappa_m]$ and the resulting equation

$$\frac{\partial \mathcal{F}^{(m)}}{\partial t} = \frac{3}{2}\frac{\mathcal{F}^{(m)}\mathcal{F}^{(m-1)}}{k^{(m)}} - \frac{3}{2}\frac{(\mathcal{F}^{(m)})^2}{k^{(m)}} \tag{A6}$$

looks like the flux equation in the multiple scale model for the spectral slice (m). It has also the very same structure as the standard dissipation-rate equation in which the coefficients are $c_{\epsilon_1} = c_{\epsilon_2} = 3/2$. Although the Kovasznay spectral hypothesis is a very rough representation of the spectral cascade, it is interesting to note that it shows some trends towards the constant value 3/2 in the limiting case of a very thin spectral slice. In this light, this value cannot be considered as a lucky haphazard.

APPENDIX B: ANALYTICAL SOLUTION OF THE ISOTROPIC SELF-SIMILAR DECAY TURBULENCE

1. Technical preliminary

Let us consider a Taylor series expansions in space for the function f

$$f(x) = f(x_0) + \sum_{n=1}^{\infty} \left(\frac{d^n f}{dx^n}\right)_{x_0} \frac{x^n}{n!}. \tag{B1}$$

The real power α of the function f can be easily derived as

$$[f(x)]^\alpha = f_0^\alpha + \alpha f_0^{\alpha_1} \left(\frac{df}{dx}\right)_{x_0} x + \left[\alpha f_0^{\alpha_1} \left(\frac{d^2 f}{dx^2}\right)_{x_0} \frac{x^2}{2} + \alpha\alpha_1 f_0^{\alpha_2} \left(\frac{df}{dx}\right)_{x_0}^2\right] \frac{x^2}{2}$$
$$+ \left[\alpha f_0^{\alpha_1} \left(\frac{d^3 f}{dx^3}\right)_{x_0} + 3\alpha\alpha_1 f_0^{\alpha_2} \left(\frac{df}{dx}\right)_{x_0} \left(\frac{d^3 f}{d^3 x}\right)_{x_0} + \alpha\alpha_1\alpha_2 f_0^{\alpha_3} \left(\frac{df}{dx}\right)_{x_0}^3\right] \frac{x^3}{6} + O(x^4), \tag{B2}$$

where $f_0 = f(x_0)$, $\alpha_1 = \alpha - 1$, $\alpha_2 = \alpha - 2$ and $\alpha_3 = \alpha - 3$. For a given series

$$f(x) = \sum_{n=0}^{\infty} a_n x^n, \tag{B3}$$

Eq. (B2) can be applied for $\alpha = 3/2$ leading to the result

$$[f(x)]^{3/2} = a_0^{3/2} + \frac{3}{2} a_0^{1/2} a_1 x + \frac{3}{2} a_0^{-1/2} \left[a_0 a_2 + \frac{1}{4} a_1^2\right] x^2$$
$$+ \frac{3}{2} a_0^{-3/2} \left[a_0^2 a_3 + \frac{1}{2} a_0 a_1 a_2 - \frac{1}{24} a_1^3\right] x^3 + O(x^4). \tag{B4}$$

2. Analytical spectrum solution

The similarity hypothesis studied in particular by Monin and Yaglom[57] (Vol. II, 16.1) leads to a separation of variables

$$E(\kappa, t) = \frac{b}{\sqrt{t}} G(\gamma), \tag{B5}$$

where $\gamma = \kappa\sqrt{at}$, a and b being constant coefficients.

Considering the variable change $(\kappa, t) \curvearrowright (\gamma, T)$ with $\gamma = \gamma(\kappa, t) = \kappa\sqrt{at}$ and $T = T(t) = t$, the previous equation shows that

$$k = \int_0^\infty E(\kappa, t) d\kappa = \int_0^\infty \frac{b}{\sqrt{t}} G(\kappa\sqrt{at}) d\kappa = \int_0^\infty \frac{b}{\sqrt{a}T} G(\gamma) d\gamma = \frac{Cte}{T}. \tag{B6}$$

In the present case, the dimensionless reduced variable involving the time is

$$z(\kappa, t) = \epsilon(t)^{-1/3} \kappa^{-2/3} t^{-1}. \tag{B7}$$

If $\kappa(t) \propto 1/\sqrt{t}$ and $\epsilon(t) \propto t^{-2}$, then this result leads to

$$\frac{d\epsilon(t)}{dt} = -2\frac{\epsilon}{t}. \tag{B8}$$

The factor 2 in the right-hand side of this equation, obviously comes from the hypothesis of self-similarity. It implies that the time evolution of ϵ is such that $\epsilon(t) = a/t^2$. From the energy decay

equation $dk/dt = -\epsilon$ one also deduces again $k(t) = a/t$. Then follow other useful relations, all of them being consequences of the self-similarity written as

$$\frac{\epsilon}{k} = \frac{1}{t}, \qquad \frac{\epsilon^2}{k} = \frac{a}{t^2}, \qquad \frac{k^{3/2}}{\epsilon} = \sqrt{a}t. \tag{B9}$$

In order to derive the solution equations of Reid and Harris[56] (solution for large values of the Reynolds number in the initial period similarity), the spectrum and the transfer term are computed by Taylor series expansions of the dimensionless variable $z = z(\kappa, t)$ where κ and t are independent variables as follows:

$$E(\kappa, t) = C_\kappa\, \epsilon(t)^{2/3} \kappa^{-5/3} \sum_{n=0}^{\infty} a_n\, z^n, \tag{B10}$$

where $a_0 = 1$. The Kovasznay hypothesis for the transfer term

$$\mathcal{F}(\kappa, t) = C_\kappa^{-3/2}\, E(\kappa, t)^{3/2}\, \kappa^{5/2} \tag{B11}$$

gives the series equation

$$\mathcal{F}(\kappa, t) = \epsilon(t) \left[\sum_{n=0}^{\infty} a_n\, z^n \right]^{3/2}. \tag{B12}$$

The spectrum E and the transfer term $\mathcal{F}$ are obtained by satisfying Eq. (69) with the theoretical assumption that the Reynolds number goes to infinity or equivalently that the fluid viscosity goes to zero. The derivatives $\partial E/\partial t$ and $\partial \mathcal{F}/\partial \kappa$ are calculated and then identified. The derivative of Eq. (B10) reads

$$\frac{\partial E(\kappa, t)}{\partial t} = C_\kappa \kappa^{-5/3} \left[\frac{2}{3} \epsilon^{-1/3} \frac{d\epsilon}{dt} \sum_{n=0}^{\infty} a_n\, z^n + \epsilon^{2/3} \sum_{n=0}^{\infty} n\, a_n\, z^{n-1} \frac{\partial z}{\partial t} \right]. \tag{B13}$$

The derivative $d\epsilon/dt$ given by Eq. (B8) is computed as

$$\frac{d\epsilon(t)}{dt} = -2\epsilon^{4/3} \kappa^{2/3} z. \tag{B14}$$

The derivative $\partial z/\partial t$ is computed using Eq. (B8) coming from the self-preservation hypothesis

$$\frac{\partial z(\kappa, t)}{\partial t} = -\kappa^{-2/3} \left[\frac{1}{3} \epsilon^{-4/3} \frac{d\epsilon}{dt} t^{-1} + \epsilon^{-1/3} t^{-2} \right] = -\frac{z}{3t} = -\frac{1}{3} \epsilon^{1/3} \kappa^{2/3} z^2. \tag{B15}$$

So that Eq. (B13) reads

$$\frac{\partial E(\kappa, t)}{\partial t} = -\frac{2}{3} C_\kappa\, \epsilon \kappa^{-1} \left[2z + \frac{5}{2} a_1 z^2 + 3a_2 z^2 + \frac{7}{2} a_3 z^3 + O(z^4) \right]. \tag{B16}$$

Using the preliminary result (B4) in Eq. (B12), one can then obtain

$$\mathcal{F}(\kappa, t) = \epsilon \left[1 + \frac{3}{2} a_1 z + \frac{3}{2} \left(a_2 + \frac{a_1^2}{4} \right) z^2 + \frac{3}{2} \left(a_3 + \frac{1}{2} a_1 a_2 - \frac{a_1^3}{24} \right) z^3 + O\left(z^4\right) \right]. \tag{B17}$$

The derivative of Eq. (B17) with respect to the wave number κ is obtained from

$$\frac{\partial \mathcal{F}(\kappa, t)}{\partial \kappa} = \frac{\partial \mathcal{F}(\kappa, t)}{\partial z(\kappa, t)} \frac{\partial z(\kappa, t)}{\partial \kappa}. \tag{B18}$$

The derivative $\partial z/\partial \kappa$ is computed using Eq. (B8) coming from the self-preservation hypothesis

$$\frac{\partial z(\kappa, t)}{\partial \kappa} = -\frac{2}{3} \kappa^{-5/3} \epsilon^{-1/3} t^{-1} = -\frac{2}{3} \frac{z}{\kappa}. \tag{B19}$$

Hence, the derivative of Eq. (B17) can be written

$$\frac{\partial \mathcal{F}(\kappa, t)}{\partial \kappa} = \frac{\partial \mathcal{F}}{\partial z} \frac{\partial z}{\partial \kappa} = -\frac{2}{3} \epsilon \kappa^{-1} \left[\frac{3}{2} a_1 z + 3 \left(a_2 + \frac{a_1^2}{4} \right) z^2 + \frac{9}{2} \left(a_3 + \frac{a_1 a_2}{2} - \frac{a_1^3}{24} \right) z^3 + O\left(z^4\right) \right]. \tag{B20}$$

By identifying term by term the series (B16) and (B20), one can easily obtain $a_1 = -4C_\kappa/3$, $a_2 = 2{C_\kappa}^2/3$ and $a_3 = -8{C_\kappa}^3/81$ so that the final results read

$$E(\kappa,t) = C_\kappa\,\epsilon^{2/3}\kappa^{-5/3} - \frac{4}{3}{C_\kappa}^2\,\epsilon^{1/3}\frac{\kappa^{-7/3}}{t} + \frac{2}{3}{C_\kappa}^3\frac{\kappa^{-3}}{t^2} - \frac{8}{81}{C_\kappa}^4\epsilon^{-1/3}\frac{\kappa^{-11/3}}{t^3} + \epsilon^{2/3}\kappa^{-5/3}O(z^4), \tag{B21}$$

$$\mathcal{F}(\kappa,t) = \epsilon - 2C_\kappa\,\frac{\epsilon^{2/3}\kappa^{-2/3}}{t} + \frac{5}{3}{C_\kappa}^2\,\frac{\epsilon^{1/3}\kappa^{-4/3}}{t^2} - \frac{2}{3}{C_\kappa}^3\,\frac{\kappa^{-2}}{t^3} + \epsilon\,O(z^4), \tag{B22}$$

$$\frac{\partial\mathcal{F}}{\partial\kappa}(\kappa,t) = \frac{4}{3}C_\kappa\,\frac{\epsilon^{2/3}\kappa^{-5/3}}{t} - \frac{20}{9}{C_\kappa}^2\,\frac{\epsilon^{1/3}\kappa^{-7/3}}{t^2} + \frac{4}{3}{C_\kappa}^3\,\frac{\kappa^{-3}}{t^3} + \epsilon\kappa^{-1}O(z^4). \tag{B23}$$

As expected, one can verify that $\lim_{t\to\infty}E(\kappa,t) = C_\kappa\,\epsilon^{2/3}\kappa^{-5/3}$ and $\lim_{t\to\infty}\mathcal{F}(\kappa,t) = \epsilon$. It is also important to remark that the first term in the right-hand side of Eq. (B22), which is the major term contribute for nothing in Eq. (69). The active term is indeed the second term in the right-hand side of Eq. (B22) which is far smaller in value. The same mechanism happens in the PITM method in which the acting mechanism comes from the $(F - \mathcal{F})$ flux difference.

APPENDIX C: THE $c_{\epsilon 2}$ COEFFICIENT FROM INTEGRATION TECHNIQUE

In statistical RANS turbulence modeling, the c_{ϵ_2} coefficient is not at all a universal constant but it depends on the spectral distribution itself, on the turbulent energy which has been transferred from the large scales to the small scales by the turbulence cascade and on the type of flow. In this respect, it is interesting to consider a schematic energy spectrum defined as follows:

$$\begin{aligned} E(\kappa) &= \alpha\kappa^m \quad for \quad \kappa \le \kappa_0, \\ E(\kappa) &= C_\kappa\,\epsilon^{2/3}\,\kappa^{-5/3} \quad for \quad \kappa \ge \kappa_0, \end{aligned} \tag{C1}$$

where m is a parameter coefficient. There is a simple way[49] (Section 5.10) to derive a decay ϵ-equation, summarized hereafter. The maximum of the spectrum is obtained for $\kappa_0 = (C_\kappa\epsilon^{2/3}/\alpha)^{3/3m+5}$. It is then simple matter to compute the turbulent energy

$$k = \int_0^\infty E(\kappa)\,d\kappa = \frac{3m+5}{2(m+1)}C_\kappa\epsilon^{2/3}\kappa_0^{-2/3} = \frac{3m+5}{2(m+1)}\,\alpha^{\frac{2}{3m+5}}\,C_\kappa^{\frac{3(m+1)}{3m+5}}\,\epsilon^{\frac{2(m+1)}{3m+5}}. \tag{C2}$$

The equation describing the law of the dissipation-rate decay can be easily obtained by taking the derivative of Eq. (C2)

$$\frac{dk}{k} = \left(\frac{2m+2}{3m+5}\right)\frac{d\epsilon}{\epsilon} \tag{C3}$$

and by considering the equation of the turbulent energy decay in absence of production, one can easily find the resulting equation

$$\frac{d\epsilon}{dt} = -\left(\frac{3m+5}{2m+2}\right)\frac{\epsilon^2}{k} \tag{C4}$$

showing clearly that the coefficient c_{ϵ_2} is a function of the parameter m that characterizes the spectrum in the zone of large scales. As a result, in the case of self-similar decay, the value $c_{\epsilon_2} = 2$ is recovered for the particular value $m = 1$.

[1] J. Fröhlich and D. Von Terzi, "Hybrid LES/RANS methods for the simulation of turbulent flows," Prog. Aerosp. Sci. **44**, 349 (2008).
[2] M. Germano, "From RANS to DNS: Toward a bridging model," in *Direct and Large-Eddy Simulation III*, ERCOFTAC Series, edited by P. Voke, N. D. Sandham, and L. Kleiser (Kluwer Academic, 1999), Vol. 7, p. 225.
[3] P. R. Spalart, "Detached-eddy simulation," Annu. Rev. Fluid Mech. **41**, 181 (2009).

[4] M. L. Shur, P. R. Spalart, M. K. Strelets, and A. K. Travin, "A hybrid RANS-LES approach with delayed-DES and wall-modelled LES capabilities," Int. J. Heat Fluid Flow **29**, 1638 (2008).
[5] T. B. Gatski, C. L. Rumsey, and R. Manceau, "Current trends in modelling research for turbulent aerodynamic flows," Philos. Trans. R. Soc. London, Ser. A **365**, 2389 (2007).
[6] M. Lesieur and O. Metais, "New trends in large-eddy simulations of turbulence," Annu. Rev. Fluid Mech. **28**, 45 (1996).
[7] P. Sagaut, S. Deck, and M. Terracol, *Multiscale and Multiresolution Approaches in Turbulence* (Imperial College Press, London, 2006).
[8] P. R. Spalart, "Strategies for turbulence modelling and simulations," Int. J. Heat Fluid Flow **21**, 252 (2000).
[9] F. Hamba, "A hybrid RANS/LES simulation of turbulent channel flow," Theor. Comput. Fluid Dyn. **16**, 387 (2003).
[10] L. Temmerman, M. Hadziabdic, M. A. Leschziner, and K. Hanjalic, "A hybrid two-layer URANS-LES approach for large eddy simulation at high Reynolds numbers," Int. J. Heat Fluid Flow **26**, 173 (2005).
[11] L. Davidson and M. Billson, "Hybrid LES-RANS using synthesized turbulent fluctuations for forcing in the interface region," Int. J. Heat Fluid Flow **27**, 1028 (2006).
[12] R. Schiestel and A. Dejoan, "Towards a new partially integrated transport model for coarse grid and unsteady turbulent flow simulations," Theor. Comput. Fluid Dyn. **18**, 443 (2005).
[13] B. Chaouat and R. Schiestel, "A new partially integrated transport model for subgrid-scale stresses and dissipation rate for turbulent developing flows," Phys. Fluids **17**, 065106 (2005).
[14] R. Schiestel, "Multiple-time scale modeling of turbulent flows in one point closures," Phys. Fluids **30**, 722 (1987).
[15] B. Chaouat, "Subfilter-scale transport model for hybrid RANS/LES simulations applied to a complex bounded flow," J. Turbul. **11**, 1 (2010).
[16] B. Chaouat and R. Schiestel, "Progress in subgrid-scale transport modelling for continuous hybrid non-zonal RANS/LES simulations," Int. J. Heat Fluid Flow **30**, 602 (2009).
[17] B. Chaouat, "Simulation of turbulent rotating flows using a subfilter scale stress model derived from the partially integrated transport modeling method," Phys. Fluids **24**, 045108 (2012).
[18] A. Fadai-Ghotbi, C. Friess, R. Manceau, T. B. Gatski, and J. Borée, "Temporal filtering: A consistent formalism for seamless hybrid RANS-LES modeling in inhomogeneous turbulence," Int. J. Heat Fluid Flow **31**, 378 (2010).
[19] A. Fadai-Ghotbi, C. Friess, R. Manceau, and J. Borée, "A seamless hybrid RANS-LES model based on transport equations for the subgrid stressses and ellipting blending," Phys. Fluids **22**, 055104 (2010).
[20] B. E. Launder, G. J. Reece, and W. Rodi, "Progress in the development of a Reynolds stress turbulence closure," J. Fluid Mech. **68**, 537 (1975).
[21] B. E. Launder and N. Shima, "Second moment closure for the near wall sublayer: Development and application," AIAA J. **27**, 1319 (1989).
[22] C. G. Speziale, "Analytical methods for the development of Reynolds-stress closures in turbulence," Annu. Rev. Fluid Mech. **23**, 107 (1991).
[23] R. Manceau and K. Hanjalic, "Elliptic blending model: A new near-wall Reynolds-stress turbulence closure," Phys. Fluids **14**, 744 (2002).
[24] S. S. Girimaji, E. Jeong, and R. Srinivasan, "Partially averaged Navier-Stokes method for turbulence: Fixed point analysis and comparisons with unsteady partially averaged Navier-Stokes," ASME J. Appl. Mech. **73**, 422 (2006).
[25] S. Jakirlic, S. Saric, G. Kadavelil, E. Sirbubalo, B. Basara, and B. Chaouat, "SGS modelling in LES of wall-bounded flows using transport RANS models: From a zonal to a seamless hybrid LES/RANS method," in *Proceedings of the 6th Symposium on Turbulent Shear Flow Phenomena*, edited by N. Kasagi, J. Eaton, R. Friedrich, J. Humphrey, A. Johansson, and H. Sung (Seoul, 2009), Vol. 3, pp. 1057–1062.
[26] D. Jeong, Y. Choi, and J. Shin, "Hybrid RANS-LES approaches for the prediction of turbulent heat flux," in *Proceedings of the 6th Symposium on Turbulent Shear Flow Phenomena*, edited by N. Kasagi, J. Eaton, R. Friedrich, J. Humphrey, A. Johansson, and H. Sung (Seoul, 2009), Vol. 2, pp. 517–522.
[27] Y. Bentaleb and R. Manceau, "A hybrid RANS/LES formulation based on a two-equation subfilter model," in *Proceedings of the 7th Symposium on Turbulent Shear Flow Phenomena*, edited by J. Eaton, R. Friedrich, J. Humphrey, A. Johanson, N. Kasagi, and S. Tavoularis (Ottawa, 2011) No. 9A4P, pp. 1–6.
[28] W. H. Reid and D. L. Harris, "Similarity spectra in isotropic turbulence," Phys. Fluids **2**, 139 (1959).
[29] J. O. Hinze, *Turbulence* (McGraw-Hill, New York, 1975).
[30] A. Craya, "Contribution à l'analyse de la turbulence associée à des vitesses moyennes," *publication scientifique et technique*, edited by Ministère de l'Air (Paris, 1958), p. 345.
[31] A. Laporta, "Etude spectrale et modélisation de la turbulence inhomogène," Ph.D dissertation (Ecole Centrale Lyon, 1996).
[32] A. Laporta and J. P. Bertoglio, "A model for inhomogeneous turbulence based on two-point correlations," *Advances in Turbulence V*, edited by R. Benzi (Kluwer Academic, 1995), pp. 286–297.
[33] B. Chaouat and R. Schiestel, "From single-scale turbulence models to multiple-scale and subgrid-scale models by Fourier transform," Theor. Comput. Fluid Dyn. **21**, 201 (2007).
[34] D. Jeandel, J. F. Brison, and J. Mathieu, "Modeling methods in physical and spectral space," Phys. Fluids **21**, 169 (1978).
[35] C. Cambon, D. Jeandel, and J. Mathieu, "Spectral modelling of homogeneous non-isotropic turbulence," J. Fluid Mech. **104**, 247 (1981).
[36] R. Schiestel and L. Elena, "Modeling of anisotropic turbulence in rapid rotation," Aerosp. Sci. Technol. **7**, 441 (1997).
[37] W. J. T. Bos and J. P. Bertoglio, "Inertial range scaling of scalar flux spectra in uniformly sheared turbulence," Phys. Fluids **19**, 025104 (2007).
[38] F. S. Godeferd, C. Cambon, and J. F. Scott, "Two-point closures and their applications: Report on a workshop," J. Fluid Mech. **436**, 393 (2001).

[39] R. Schiestel, "Sur le concept d'échelles multiples en modélisation des écoulements turbulents. Part I," J. Theor. Appl. Mech. **2**, 417 (1983).
[40] R. Schiestel, "Sur le concept d'échelles multiples en modélisation des écoulements turbulents. Part II," J. Theor. Appl. Mech. **2**, 601 (1983).
[41] A. Cimarelli and E. De Angelis, "Analysis of the Kolmogorov equation for filtered wall-turbulent flows," J. Fluid Mech. **676**, 376 (2011).
[42] C. Cambon, C. Teissedre, and D. Jeandel, "Etude d'effets couplés de déformation et de rotation sur une turbulence homogène," J. Theor. Appl. Mech. **4**, 629 (1985).
[43] J. Mathieu, D. Jeandel, B. E. Launder, W. C. Reynolds, and W. Rodi, *Simulation of Turbulence Models and Their Applications* (Eyrolles, Paris, 1984), Vol. 1.
[44] P. Sagaut and C. Cambon, *Homogeneous Turbulence Dynamics* (Cambridge University Press, 2008).
[45] M. Lesieur, *Turbulence in Fluids*, 4th ed. (Springer, Dordrecht, 2008).
[46] S. C. Kassinos and W. C. Reynolds, "A structure based model for the rapid distorsion of homogeneous turbulence," Thermoscience Division, Department of Mechanical Engineering, Report No. TF-61, Stanford University, USA, 1994.
[47] C. Cambon, L. Jacquin, and J. L. Lubrano, "Toward a new Reynolds stress model for rotating turbulent flows," Phys. Fluids **4**, 812 (1992).
[48] A. Yoshizawa, "A statistically-derivated subgrid model for the large-eddy simulation of turbulence," Phys. Fluids **25**, 1532 (1982).
[49] R. Schiestel, *Modeling and Simulation of Turbulent Flows* (ISTE/Wiley, 2008).
[50] R. Schiestel and B. Chaouat, "On partially integrated transport models for subgrid-scale modelling," ERCOFTAC Bull. **72**, 49 (2007).
[51] M. Germano, "Turbulence: the filtering approach" J. Fluid Mech. **238**, 325 (1992).
[52] L. C. Berselli, T. Iliescu, and W. J. Layton, *Mathematics of Large Eddy Simulation of Turbulent Flows* (Springer, Berlin, 2006), pp. 227–251.
[53] F. Hamba, "Analysis of filtered Navier-Stokes equation for hybrid RANS/LES simulation," Phys. Fluids **23**, 015108 (2011).
[54] A. Scotti, C. Meneveau, and D. K. Lilly, "Generalized Smagorinsky model for anisotropic grids," Phys. Fluids **5**, 2306 (1993).
[55] S. S. Girimaji and R. Rubinstein, "Two-point turbulence closure applied to variable resolution modeling," AIAA Paper 2011-3470, 2011.
[56] W. H. Reid and D. L. Harris, "The similarity spectra in isotropic turbulence using Kovasznay's form of the transfer function," Technical Report No. 17, 1958, Office of Naval Research, Division of Applied Mathematics, Brown University, Providence, RI, 1958.
[57] A. S. Monin and A. M. Yaglom, *Statistical Fluid Mechanics* (MIT, Cambridge, MA, 1975).
[58] W. J. T. Bos, L. Shao, and J. P. Bertoglio, "Spectral imbalance and the normalized dissipation rate of turbulence," Phys. Fluids **19**, 045101 (2007).
[59] W. P. Jones and B. E. Launder, "The prediction of laminarization with a two-equation model of turbulence," Int. J. Heat Mass Transfer **15**, 301 (1972).
[60] B. E. Launder and B. I. Sharma, "Application of the energy dissipation model of turbulence to the calculation of flow near a spinning disc," Lett. Heat Mass Transfer **1**, 131 (1974).
[61] P. A. Durbin, "A Reynolds stress model for near-wall turbulence," J. Fluid Mech. **249**, 465 (1993).
[62] C. G. Speziale, S. Sarkar, and T. B. Gatski, "Modelling the pressure-strain correlation of turbulence: An invariant dynamical systems approach," J. Fluid Mech. **227**, 245 (1991).
[63] F. R. Menter, M. Kuntz, and R. Langtry, "Ten years of industrial experience with the SST turbulence model," in *Turbulence, Heat and Mass Transfer*, edited by Y. Nagano, K. Hanjalic, and M. Tummers (Begell House, Redding, CT, 2003), Vol. 4, pp. 625–632.
[64] S. C. Crow, "Viscoelastic properties of the fine-grained incompressible turbulence," J. Fluid Mech. **33**, 1 (1968).
[65] C. Cambon and L. Jacquin, "Spectral approach to non-isotropic turbulence subjected to rotation," J. Fluid Mech. **202**, 295 (1989).
[66] S. C. Kassinos, C. A. Langer, S. L. Haire, and W. C. Reynolds, "Structure-based turbulence modelling for wall bounded flows," Int. J. Heat Fluid Flow **21**, 599 (2000).
[67] C. Cambon and B. Chaouat, "Refined modelling in terms of directional anisotropy and polarization anisotropy for coupled effects of strain and rotation," in *Proceedings of the* 10*th Engineering Turbulence Modelling and Measurements*, edited by M. A. Leschziner, P. Bontoux, B. J. Geurt, B. E. Launder, and C. Tropea (Marseille, 2010), Vol. 2, pp. 552–557.
[68] B. Chaouat, "An efficient numerical method for RANS/LES turbulent simulations using subfilter scale stress transport equations," Int. J. Numer. Methods Fluids **67**, 1207 (2011).
[69] G. Comte-Bellot and S. Corrsin, "Simple Eulerian time correlation of full and narrow-band velocity signals in grid-generated, isotropic turbulence," J. Fluid Mech. **48**, 273 (1971).
[70] I. Befeno and R. Schiestel, "Non-equilibrium mixing of turbulence scales using a continuous hybrid RANS/LES approach: Application to the shearless mixing layer," Flow, Turbul. Combust. **78**, 129 (2007).
[71] C. Rapp and M. Manhart, "Flow over periodic hills: An experimental study," Exp. Fluids **51**, 247 (2011).